"Određivanje sadržaja karotenoida hridinskog ježinca, Paracentrotus lividus uz pomoć Raman spektroskopije"

Nekvapil, Fran

Master's thesis / Diplomski rad

2017

Degree Grantor / Ustanova koja je dodijelila akademski / stručni stupanj: **University of Dubrovnik / Sveučilište u Dubrovniku**

Permanent link / Trajna poveznica: https://urn.nsk.hr/urn:nbn:hr:155:019677

UNIVERSITY OF DUBROVNIK

DEPARTMENT OF AQUACULTURE

MASTER DEGREE STUDY PROGRAMME MARICULTURE

Fran Nekvapil

Quantification of carotenoids in the stony sea urchin *Paracentrotus lividus* Lamarck 1816

MASTER THESIS

Dubrovnik, 2017

UNIVERSITY OF DUBROVNIK

DEPARTMENT OF AQUACULTURE

MASTER DEGREE STUDY PROGRAMME MARICULTURE

Fran Nekvapil

Quantification of carotenoids in the stony sea urchin *Paracentrotus lividus* Lamarck 1816

MASTER THESIS

Supervisor:

doc. dr. sc. Sanja Tomšić

Co-supervisor:

Conf. dr. Simona Cintă Pinzaru

Dubrovnik, 2017

This master thesis has been conducted under the supervision of doc. dr. sc. Sanja Tomšić, within the Master degree study programme Mariculture at the Department of Aquaculture of the University of Dubrovnik.

Part of the experimental results reported in this thesis has been obtained during the Erasmus+ mobility for traineeship within the Raman-SPM laboratory of Biomolecular Physics Department of Babeș-Bolyai University In Cluj-Napoca, Romania, under the supervision of Conf. dr. Simona Cintă Pinzaru.

CONTENTS

ACKNOWLEDGEMENTS

First and foremost, I express my enormous gratitude to Conf. dr. Simona Cintă Pinzaru, my Erasmus coordinator and co-supervisor for the present thesis. Her all day long concern about me and my work, be it regarding this thesis or other research, is highly appreciated. Her guidance through the world of science was invaluable. She is the soul of the research described here.

Special thanks to my supervisor doc. dr. sc. Sanja Tomšić. I value her guidance and support in conducting the present research and preparation of the thesis very much. She is a great teacher and a great supervisor.

Great thanks to the Department of Aquaculture at the University of Dubrovnik, and to all its employees. The Department provided facilities and equipment for initial preparation of the samples.

Department of Biomolecular Physics of the Babeș-Bolyai University in Cluj-Napoca, Romania, is also greatly thanked to for providing equipment and facilities where a part of here described research has been conducted.

I also express my great gratitude to my family, especially to my parents, dr. vet. med. Sandra Prevendar-Nekvapil and dipl. ing. Ivan Nekvapil, for their continuous support and understanding, throughout my studies.

I would also like to express my gratitude to M.sc. Ioana Brezestean, for her understanding, patience and great help in sample preparation, analysis itself and help with getting familiar with various laboratory Instruments and procedures.

Lucian Barbu-Tudoran, Ph.D. is also thanked, for producing high-quality scanning electron micrographs, which were used to support this and related studies.

I cannot forget to thank my friends at all levels of study, and all former supervisors, for their input also played a part in the development of my scientific personality and interests.

Quantification of carotenoids in the stony sea urchin, *Paracentrotus lividus* Lamarck 1816

ABSTRACT

This thesis presents some data from a series on studies where Raman spectroscopy was used to acquire molecular information from selected marine organisms. In fact, the main mission of the present thesis is to demonstrate the capability and versatility of Raman spectroscopy, and hence its potential utility in marine biology basic or applied research. This will be achieved through presenting a part of our results dealing with the stony sea urchin, *Paracentrotus lividus*. Raman spectroscopy was capable to detect multiple carotenoid species in soft tissues of *P. lividus* life stages and body parts (gonads, eggs, larvae, gut), as well as to characterize the hard tissues (larval skeleton, spines) as being calcite with ipossible nclusions of magnesium and amorphous calcium carbonate. The thesis also opens new avenues and challenges to further develop Raman spectroscopic analysis of samples from marine environment.

Keywords: Raman spectroscopy, stony sea urchin, carotenoids, gonads, eggs, digestive system

Kvantifikacija karotenoida u hridinskom ježincu, *Paracentrotus lividus* Lamarck 1816

SAŽETAK

Ovaj rad iznosi neke podatke iz slijeda istraživanja odabranih morskih organizama koristeći Raman spektroskopiju za dobivanje molekularnih informacija o uzorcima. U stvari, zadatak ovoga rada je bio pokazati mogućnosti i prilagodljivost Raman spektroskopije, te tako i potencijalnu upotrebljivost ove metode u osnovnim i primijenjenim istraživanjima u biologiji mora. To će se postići predstavljenjem dijela naših rezultata koji se tiče hridinskog ježinca, *Paracentrotus lividus*. Raman spektroskopijom smo mogli detektirati više vrsta karotenoida u mekim tkivima hridinskog ježinca i nekim njegovim razvojnim stadijima (u gonadama, jajnim

stanicama, ličinkama, dijelovima probavnog sustava) te utvrditi da se tvrda tkiva (skelet ličinki, bodlje) sastoje uglavnom od kalcita s mogućim uklopinama magnezija i amorfnog kalcijevog karbonata. Ovaj rad također otvara nove smjerove i izazove za daljnji razvoj Raman spektroskopije kao metode za analizu uzoraka iz morskog okoliša.

Ključne riječi: Raman spektroskopija, hridinski ježinac, karotenoidi, gonade, jajne stanice, probavni sustav

1. INTRODUCTION

Carotenoids are secondary metabolites synthesized by plants and algae to perform a wide range of functions in these organisms (Shumskaya and Wurtzel, 2013). Carotenoids also have many beneficial effects for humans when acquired through carotenoid-rich plant-based food: protection of the skin against external and internal hazards (Darvin, et al., 2011), protection against age-related macular degeneration (Meyers et al., 2014), protection against tumours (Nishino et al., 2000) and many other. There are more than 600 carotenoid species known in nature, many of which are specific to certain species (Kiokias et al., 2016).

High performance liquid chromatography (HPLC) has often been used to characterise carotenoid pigments in marine environment. For instance, carotenoid pigments were identified by means of HPLC in phytoplankton (Ahel and Tezić, 1998; Flander-Putrle, 2010; Leruste et al., 2015), macroalgae (Sugawara et al., 2002), sea urchins (Liyana-Pathirana et al., 2002; Shpigel et al., 2006; Symonds et al., 2007; Symonds et al., 2009; Garama et al., 2012), to name just some studies.

However, the preparation of carotenoids for HPLC analysis can comprise several steps, with extraction and dissolution of carotenoids being mandatory. The HPLC analysis, including sample preparation, can be time-consuming, costly, a portion of carotenoids could be lost during sample preparation, and it is limited to laboratory analysis. In contrast, Raman spectroscopy is fast, cost-effective, precise, the sample preparation may be very reduced and the method is non-destructive. Our studies support these advantages. Firstly, we were able to get information on carotenoids in our samples in a matter of seconds. Furthermore, we spent very few consumable materials (just some pipette tips, a few test tubes, few ml of ethanol, etc.). Preparation of samples was usually limited to physically shaping to fit under microscope objectives or dropping solutions on microscope slides. The non-destructive character of Raman spectroscopy is very useful for monitoring chemical changes on the same spot over time.

Raman spectroscopy has also been used to characterize organisms from the marine environment, For instance, Kaczor and Baranska (2011) and Cintă Pinzaru et al. (2016) analysed a species of alga, Salares et al. (1977), Katsikini (2016) and Nekvapil et al. (manuscript in preparationn) analysed the native shells of

crustaceans, and Cintă Pinzaru et al. (2015) analysed sea urchin gonads for carotenoids.

1.1. Raman spectroscopy

1.1.1. Basic principles of Raman spectroscopy

The explanation of the basic principle of Raman spectroscopy was given in more detail by Smith and Dent (2005). Here those principles are simplified and described in a few sentences to give the reader enough information to be able to follow the present thesis.

Photons that make up the light can interact with matter in several ways. In Raman spectroscopy, we are interested in the process of Raman scattering, also called “inelastic scattering”. Raman spectroscopy uses the radiation of single frequency (laser) to irradiate the sample, and it is the radiation scattered from the molecules, with different energy relative to the incident radiation, that is detected.

In Raman spectroscopy, the light interacts with the molecule and distorts the cloud of electrons around the nuclei to create a short-lived state called the “virtual state”. This state is not stable and the photon is quickly re-radiated. In Raman scattering, the energy is transferred either from the photon to the molecule or from the molecule to photon. It is inherently a weak process and only one in 10^6 to 10^8 scattered photons is Raman scattered.

Figure 1 shows the basic processes that occur during inelastic scattering. At room temperature, most molecules are present in the lowest energy vibrational level. The Raman scattering process leads to absorption of energy by the molecule and its promotion from the ground vibrational state *m* to a higher energy vibrational state *n*. Some molecules will be present in the higher energy vibrational state *n* prior to interaction with photons, and in that case after interaction with the photons and promotion to the virtual state, the energy will be transferred to the photons and these molecules will return to their ground energy vibrational state *m*.

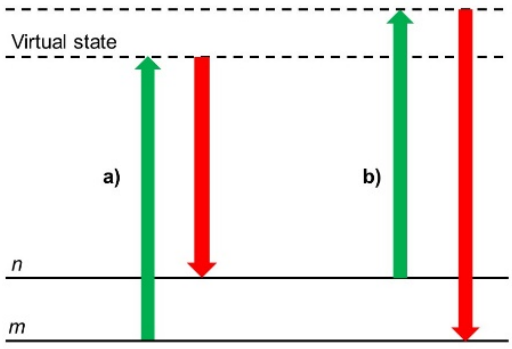

Figure 1. Diagram of the processes occurring during Raman scattering. In a) the molecules are in their ground energy state *m*, and upon absorbing a photon pass through the virtual state and return to a higher energy vibrational state *n*. In b) the molecules are in a higher energy vibrational state *n*, and upon interaction with the photons pass through the virtual state and return to their ground energy vibrational state *m*.

1.1.2. Resonance Raman scattering

Resonance Raman scattering (RRS) is a technique for selective enhancement of Raman signals of certain groups of molecules. The precondition for a molecule to be enhanced by RRS is having a chromophore. The chromophore is a chemical structure that can absorb photons. Using RRS it is possible to obtain enhancements as high as 10^6 times, but enhancements of 10^3 times are often observed. The absorbed energy is lost from the molecules through transferring it to the lattice or through emitting fluorescence. The RRS effect is observed when the energy of the laser used for excitation approaches the electron transition (maximum absorption wavelength) of the target molecule. It is not necessary to use the laser of the wavelength exactly matching the maximum absorption of the molecule, but the resonance effect is greater as the laser wavelength approaches it (Smith & Dent, 2005). The resonance wavelength of a molecule can be easily determined by acquiring its UV/Vis electronic absorption spectrum.

The study that we conducted on the shell of *Callinectes sapidus* (Nekvapil et al., manuscript in preparation) is a prime example of importance of using excitation line resonant to target compound in biological samples composed of many different

molecules. When the *C. sapidus* shell was excited with 532 nm laser line, which is resonant to free carotenoids, the signals of carotenoids dominated the spectrum, with only weak signals from $CaCO_3$ visible apart from carotenoids. When the same area was excited with 632,8 nm laser line, which is resonant to astaxanthin-crustacyanin complexes, strong signals from those complexes dominated the spectrum and again only weak $CaCO_3$ signals were observed. Finally, when infrared laser lines were used for excitation (785, 830 and 1064 nm), $CaCO_3$ signals were dominant, while signals of carotenoids and astaxanthin-crustacyanin complexes were merely of medium strength or weak. More relevant to present study, since carotenoids usually absorb in the 460 to 490 nm range (explained later), their signals were always observed when samples were excited with the 532 nm laser line.

1.1.3. Surface-Enhanced Raman Scattering (SERS)

Raman signal of dissolved substances of low concentration can be enhanced up to 10^6 times by adsorbing them on rough metal surfaces. Such surfaces can be either metal surfaces roughened by series of oxidations and reductions or lithographic etching, or metal nanoparticles of uniform size. Silver, gold and copper have proven to be the best substrates for SERS. The most important physical characteristic of prepared substrate for SERS experiments is a single repeating roughness feature (in case of larger pieces of metal) or the uniform size of nanometre scale (in case of nanoparticles). The SERS effect is not fully explained – the largest knowledge gap is that regarding the mode of adsorption of organic molecules to metal surfaces. However, it is recognised that the surface plasmon (collective oscillation of surface electrons) of metals plays an important role in enhancement of Raman signals (Smith & Dent, 2005).

We used the silver nanoparticles (AgNPs) of the size of about 20 nm in our experiments. Since very low amount of analyte is necessary for SERS effect to be visible, we were not able to record SERS signals from some *P. lividus* tissues because the tissue concentration of carotenoids was too high. In such cases SERS signals were completely covered by ordinary Raman signals. Cintă Pinzaru et al. (2015) tested the sensitivity of SERS method on carotenoids in ethanol extract from

P. lividus gonads. The latter authors have shown that the amount of carotenoids as low as 0.0549 µmol can be detected.

1.1.4. *The Raman spectrum*

The figure 2 shows a typical Raman spectrum of a *P. lividus* egg. The x axis is measured in "cm^{-1}", and represents the continuous range of photon energy shift. The size of the x axis can vary considerably depending on the spectral range recorded. The y axis is measured in "arbitrary units", and is related to the amount of scattered photons recorded by the detector for each wavenumber position. A "band" is a signal caused by a specific molecular vibration mode which scattered the photons. The "background" is what the word suggests – a background level of signal above which the bands arise. As a general rule, a band is considered to be an actual Raman signal if its intensity above the background is at least three times higher than the intensity of variation of noise. If there are many other scattering molecules in the sample, and their signals rise the background so much that it covers all other bands and no discrete bands are visible, then this phenomenon is called "fluorescence".

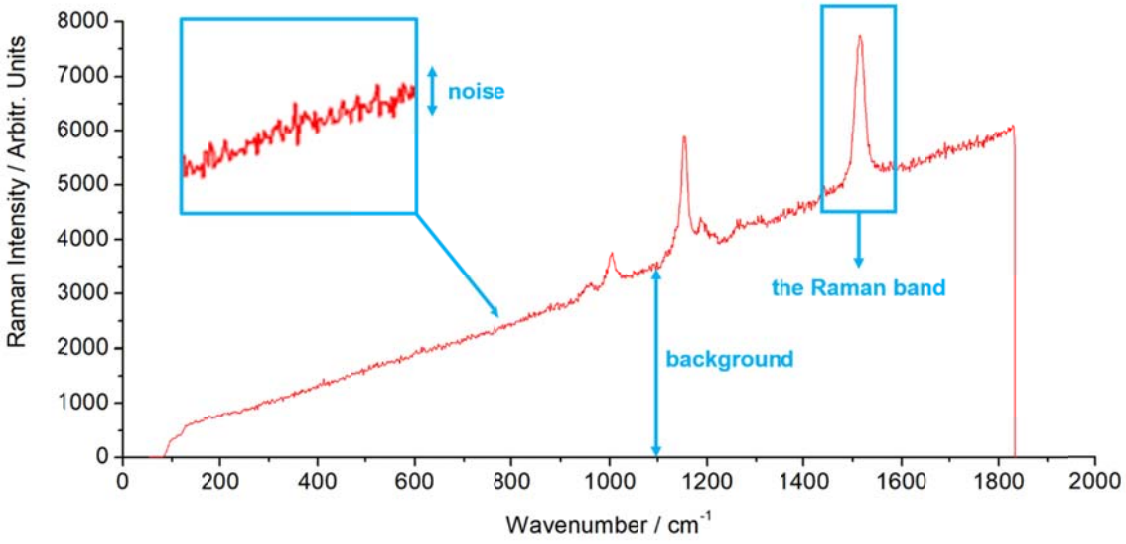

Figure 2. A representative Raman spectrum of a *Paracentrotus lividus* egg. The basic features of the Raman spectrum and graph are labelled.

1.2. Quantitative Raman spectroscopy

Raman spectroscopy can be used to determine the quantity of molecules in solid sample or liquids. The intensity of Raman bands of a particular molecular vibration is proportional to its concentration. In ordinary Raman measurements, signal intensity increases linearly with the concentration of the analyte (AZoM, 2013). On the other hand, in SERS the signal intensity increases up to SERS substrate saturation concentration, and then signal intensity relative to concentration decreases afterwards (Cintă Pinzaru et al., 2015). Many various considerations that have to be taken into account when attempting to conduct quantitative Raman analysis are outlined by Smith & Dent (2005).

1.3. Carotenoids in Raman spectroscopy

Carotenoids are very interesting for investigation with Raman spectroscopy. Because of having a chromophore, their signals often appear even when excited with laser line that is far from their absorption maximum (Merlin, 1985). However, the intensity of their signal increases dramatically as the laser line used approaches the resonance wavelength, which is usually between 460 and 490 nm (Wright & Jeffrey. 1987; Craft & Soares, 1992; Liyana-Pathirana et al., 2002; Sugawara et al., 2002; Subramanian et al., 2012; Cintă Pinzaru et al., 2015). The presence of carotenoids can be inferred from the spectra by the three major bands termed v_1, v_2 and v_3. The v_1 band is caused mainly by C=C double bond stretching, and is centred near 1515 cm^{-1}. The v_2 band is caused by a combination of C-C single bond vibration and C-H in-plane bending, and is centred near 1150 cm^{-1}. The band near 1005 cm^{-1} is termed v_3, and is caused by C-CH_3 methyl in-plane rocking. This three bands are characteristic for all carotenoids. However, their wavenumber positions in a particular carotenoid are influenced by the geometrical conformation of the carotenoid, aggregation and solvent (Merlin, 1985; Subramanian et al., 2012; Macernis et al., 2014). The proposed assignment of all carotenoid Raman bands, using *β*-carotene as an example, is presented in Table 1.

Table 1. FT-Raman and SERS data / cm^{-1} of *β*-carotene with the proposed assignment (from Cintă Pinzaru et al., 2015).

FT-Raman **β-carotene, solid, polycrystalline** **(1064 nm)**	**SERS (group a)** **(0.21 μM, 532 nm)**	**SERS (e)** **(1 μM, 532 nm)**	**Vibrational assignments*[13-15]**
	3214 w-m	3214 w	v(O-H) colloidal water
		2984 w	v(C-H)
2918 vw	2931 w	2931 w-m	v(C-H)
2850 vw	2850 w	2877 w	v(C-H)
2741 vw			v(C-H)
2667 w		2677 w	$v_1 + v_2$
		2527 w	$v_1 + v_3$
2310 w		2312 w	$2v_2$
		2162 w	$v_2 + v_3$
-	**1649 vs**		C=C cyclohexene ring
1622 vw, sh	1622 w-m increases with concentration	1622 w	v(C=C) cyclohexene ring
1585 w	1575 -1583 m		v(C=C) center of polyene chain
1512 vs	**1512 vs**	**1521 vs**	**v_1(C=C)** polyene backbone
1440 w	1445 vw	1455 w-m	asym. $\delta(CH_3)$
1392	1392 sh	1384 w	sym. $\delta(CH_3)$
1351	**1367 vs**		$\rho(CH_3)$+sym $\delta(CH_3)$
1312	1308 m		v(C=C) center of polyene chain
1279	1285 w	1279 w	ρ(C-H)
1267 w-m	1267 m		ρ(C-H)
1247 vw	1253 w		ρ(C-H)
1210 m	1226 w		v(C-C) polyene + v(C=C) centre
1189 m	1196 w- m	-	v (C-C) polyene chain

1155 vs	1179 m, 1154 vw	1156 shoulder	v_2(C-C) center
	1131 s		v (C-C) cyclohexene ring
	1083 m		v (C-C) cyclohexene ring
1006 m	1037 w	1006 m	ρ(C-CH_3) also known as "v3"
956 vvw	956 w	958 w	v (C-C)+ ρ(CH_2) +ρ(CH_3)
891 vw	881 w		modes with no theoretical Raman predictability (very low intensity)
870 vw	877 w		
851 vw	836 w		
	771, 614,		Raman forbidden modes, SERS active, cyclohexene rig def.
517 vw	493		deformation modes
371 vw	387 w		deformation modes
289 vw	291 w		deformation modes

Previous analyses of plant tissues for carotenoids point out that the wavenumber position of the v_1 band (and possibly other bands) is influenced by the length and terminal substituents of their polyene chain, and by interaction of carotenoids and molecules from surrounding matrix (Schulz et al., 2005; de Oliveira et al., 2009). Since all carotenoids have similar major Raman features, it is necessary to look for differences in minor spectral features if one wants to identify the carotenoid species in a complex sample. The region from 1100 to 1400 cm^{-1} is called "the fingerprint region", and its features are sensitive to terminal substituents and conformational changes. Thus, this area can be used for identification of carotenoid species and for their structural studies (Merlin, 1985). In addition, our related studies on carotenoid pigments in marine organisms or as reference chemicals have shown that there are difference in the presence or absence of some minor Raman bands among several kinds of carotenoids. For instance, *β*-carotene exhibits an additional weak band near 1585 cm^{-1}, while fucoxanthin exhibits its specific bands near 1610 and near 1930 cm^{-1}. Literature reports on carotenoid profile

of a sample (usually obtained by HPLC in conjunction with UV/Vis absorption spectroscopy) can help in interpretation of carotenoid Raman signal of the sample.

1.4. Calcium carbonate in Raman spectroscopy

Raman signals of calcium carbonate were readily detectable in mineralised tissues of *P. lividus*, so some of its properties deserve to be mentioned in the introduction. Calcium carbonate is most often present in three kinds of crystals – calcite, aragonite and vaterite - or as amorphous $CaCO_3$. The three crystalline phases are in fact chemically the same compound, but they can be well differentiated by Raman spectroscopy (Behrens et al., 2013), and spectra of all ordered crystalline phases are different from spectrum of amorphous $CaCO_3$ (Wang et al., 2012). As will be described in the Results chapter, we have detected only calcite phase in mineralised tissues of *P. lividus*. Raman spectrum of optically clear natural calcite was reported by Perin et al. (2016), and the spectrum of synthetic calcite was reported by Behrens et al. (2013). In short, Raman spectra of calcite usually feature six bands, termed T, L, v_4, v_1, v_3 and $2v_2$. These bands are positioned at 155.5, 282, 711.8, 1086, 1435.6 and 1748.7 cm^{-1}, respectively, in optically clear natural calcite, and only the T, L, v_4 and v_1 were recorded in synthetic calcite by Behrens et al. (2013), positioned at 155, 282, 711 and 1085 cm^{-1}, respectively. The Raman spectrum of amorphous $CaCO_3$ features only v_4 and v_1 bands, centred around 714 and 1080 cm^{-1}, respectively, and no lattice vibrations (T and L bands) can be observed (Wang et al., 2012).

1.5. Carotenoids in the stony sea urchin, *Paracentrotus lividus*

P. lividus is a common species of sea urchins in littoral areas of the study area, the southeast coast of the Adriatic Sea (Tomšić et al., 2010). It is a bottom dwelling marine invertebrate that feeds predominantly on plant matter. The species`ecology was extensively reviewed by Boudouresque and Verlaque (2013).

P. lividus has a commercial value in Europe because of its gonads (called „roe“), which are consumed as a delicacy. Stony sea urchin roe is consumed all over the Mediterranean sea and north Atlantic Ocean coasts (Fernández-Boán et al.,

2012; Matisori et al., 2012; Furesi et al., 2014). According to Furesi et al. (2014), the average consuption of roe in Sicily is as much as about 1.1 kg per capita. The preferred form for consumption appears to be raw and fresh, but roe can also be prepared with a variety of dishes, including with pasta, on pizza, or other creative combinations (Furesi et al., 2013). For this reason – *P. lividus* roe being a usual part of the diet of many people living in coastal areas - there is a inherent and biological interest in learning as much as possible about its chemical components.

High performance liquid chromatography (HPLC) alone, or in conjunction with UV/Vis absorption spectroscopy, has previously been employed to identify and quantify carotenoids in *P. lividus* gonads (Shpigel et al., 2006; Symonds et al., 2007). This was also done with some other herbivorous sea urchin species, like *Evechinus chloroticus* (Garama et al., 2012; Pilbrow et al., 2014), *Strongylocentrotus droebachiensis* (Liyana-Pathirana et al,. 2002) and *Psammechinus miliaris* (Symonds et al., 2009). These studies have identified *9`-cis*-echinenone as the most abundant carotenoid species, followed by all-*trans*-echinenone and several other carotenoids in lower quantities. In addition, Pilbrow et al. (2014) isolated a carotenoprotein which mostly has echinenone as prosthetic group. An attempt has also been made to characterize *P. lividus* gonad carotenoids using Raman spectroscopy (Cintă Pinzaru et al., 2015). In this case, the *β*-carotene has been identified and quantified, but no characteristic signals attributable to echinenone were reported.

In addition, there might be some issues with the degree of representativeness of HPLC as a detection and identification tool: HPLC demands extensive sample preparation, at least grinding or homogenisation and dissolution in several solvents. The preparation of carotenoids for HPLC analysis is therefore labour intensive, and alteration of native state of carotenoids could occur to some extent. Raman spectroscopy, on the other hand, as will be seen from the remainder of the present thesis, bypasses all those preparation steps and it is possible to analyse samples in their native state.

Carotenoid profile of *P. lividus* eggs, spent ovaries and testes have been investigated using chromatographic methods by de Nicola and Goodwin (1954). According to their analysis, eggs contain mostly *β*-carotene, echinenone and two

carotenoids named by the researchers „Paracentrotin A and B“. Spent ovaries and testes also contain mainly *β*-carotene and echinenone, but no Paracentrotins A and B. The researchers also detected some other carotenoids, but they were not unambiguously identified in the reported work. To our best knowledge, no recent study dealing with carotenoid profiles in *P. lividus* that distinguished eggs and spent gonads exists.

It seems that the carotenooid profile of *P. lividus* gonads and eggs is quite stable, regardless of dietary carotenoids. Shpigel et al. (2008) found no change in carotenoid profile of *P. lividus* gonads after 8 weeks of feeding with experimental diets including various carotenoid species as feed supplement. In contrast, Cirino et al. (2017) succeded to significantly increase astaxanthin content in *Arbacia lixula* eggs, while Peng et al. (2012) increased the content of astaxanthin in *Anthocidaris crassispina* gonads using artificial feeds.

The digestive system of *P. lividus* should contain mainly fucoxanthin, *β*-carotene, lutein and zeaxanthin, and their degradation products (Shpigel et al., 2006; Symonds et al., 2007). It would be natural to first think about carotenoids that can be found in algae on which *P. lividus* feeds. However, Shpigel et al. (2006) and Symonds et al. (2007) claim that gut carotenoid profile of *P. lividus* does not necessarily have to reflect the carotenoid profile of its food. It is believed that the gut is the site of carotenoid metabolism and that *β*-carotene is used as a precursor for synthesis of many other carotenoids (Symonds et al., 2009). The carotenoids in the studies mentioned above were characterized by means of HPLC, and to our knowledge, no Raman studies of *P. lividus* digestive system have been published.

The hollow area inside the sea urchin test is filled by biological solution called the coelomic fluid. Suspended in the coelomic fluid are the cells called the coelomocytes, which perform various tasks. According to Arizza et al. (2007), some components of coelomic fluid and coelomocytes play important role in microbiological defense of sea urchin organisms. To our best knowledge, carotenoids in *P. lividus* coelomic fluid have not yet been characterized at all. However, Liyana-Pathirana et al. (2002) published a detailed biochemical characterization of *Strongylocentrotus droebachiensis* coelomic fluid. S*. droebachiensis* is predominantly herbivorous, like *P. lividus*, but lives in north Pacific

and north Atlantic waters. According to Liyana-Pathirana et al. (2002), the carotenoid content of dry coelomic fluid is about 3.7 mg per g of tissue. Thin layer chromatography separated crude carotenoid extract into seven fractions. The dominant carotenoids were shown to be *β*-carotene and fucoxanthin, while minor carotenoids were astaxanthin, canthaxanthin and other.

According to a review by Tsushima (2013), sea urchin spines and the test should contain pigments carotenoids and naphthoquinone. The Raman spectra of carotenoids will be discussed in greater detaill in Results chapter, and the Raman spectra of some derrivatives of naphthoquinone have been reported by Umadevi et all. (2003), Singh et al. (2010) and Geetha et al. (2015). To our knowledge, there is no Raman spectroscopy analysis of naphthoquinones in sea urchin spines published thus far.

1.6. Goals of the present study

The general goal of our study is to demonstrate that Raman spectroscopy can be developed in a powerful and rapid method for investigation of samples from marine environment. This is achieved using the sea urchin *P. lividus* as a model organism. Here we attempted to characterise carotenoids (and $CaCO_3$ crystalline phase, if possible) in *P. lividus*

- gonads (both male and female)
- eggs
- larval body tissue and skeleton
- spines
- pieces of digestive systems and intestine
- coelomic fluid
- sea urchin individual as a whole

2. MATERIALS AND METHODS

2.1. The Raman spectrometers

2.1.1. Renishaw InVia Reflex Raman confocal microscope

Raman signals from solid samples or dried solutions and extracts were collected using a Renishaw InVia Reflex Raman confocal microscope (Figure 3). The light pathway during Raman measurements is schematically shown in Figure 3a. This system is a Renishaw Raman spectrometer (Figure 3d) coupled with Leica microscope (Figure 3b). The system we used was equipped with six laser lines, two ultraviolet, two in visible range, and two near-infrared (Figure 3c).

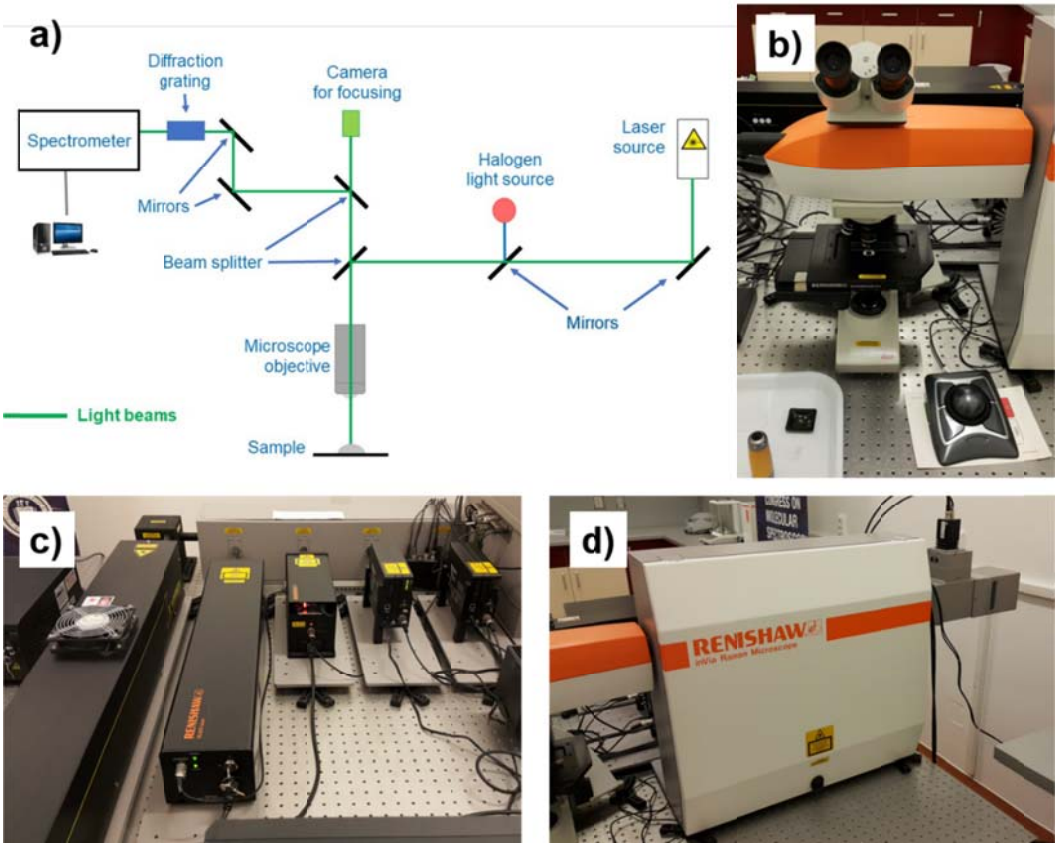

Figure 3. Workings of the Renishaw InVia Reflex Raman confocal microscope. a) simplified diagram of light pathway during Raman measurements, b) Leica research grade confocal microscope, c) the lasers – from left to right: combined 325 and 442 nm, 632.8 nm, 532 nm, 785 nm, 830 nm, d) Renishaw spectrometer.

The instrument offers possibilities to adjust wide range of spectral acquisition conditions. We were most commonly adjusting spectral range to be acquired, integration time (how long is the sample exposed to laser), number of acquisitions per spectrum (averaging more spectra) and laser power reaching the sample. The microscope used also featured several objectives, from 5x magnification to 100x. We were also changing the laser line used. The precision of spectral recording is very high on this device – the spectral resolution was 0.5 cm^{-1}, and the spatial resolution (diameter of laser spot which excites the sample) can be less than 1 μm. The instrument is capable of measuring Raman signals in a wide range in anti-Stokes. However, it was not practical to routinely record a large spectral range. Rather, a target range could be recorded. Alternatively, an extended scan covering a range 3100 cm^{-1} wide could be run, but this procedure was considerably longer (about 7 to 10 minutes per extended spectrum vs. ≈ 5 s for short range acquisition). For this reason, we did not run extended scans often. Spectra were acquired using WiRE™ 3.4 software (Renishaw, United Kingdom), they were stored in ASCII text format and processed further in Origin 6.1 software (OriginLab, USA).

2.1.2. DeltaNU Advantage 532 compact dispersive Raman spectrometer

Liquid samples and extracts were analysed on DeltaNU Advantage 532 compact dispersive Raman spectrometer (Figure 4). This device offers less freedom in setting of acquisition conditions. It records Raman signals in the range from 200 to 3500 cm^{-1} with the spectral resolution of 8 cm^{-1}. We used only the 532 nm laser line in all of our analyses and we did not change the laser power. The only conditions which we were adjusting were integration time and number of acquisitions per spectrum. The software “NuSpec” (Intevac, USA) was used to operate the device, and acquired data were stored as ASCII text files and were later processed in the Origin 6.1 software. We decided to use this device for some measurements because it is convenient to analyse the liquid samples on it.

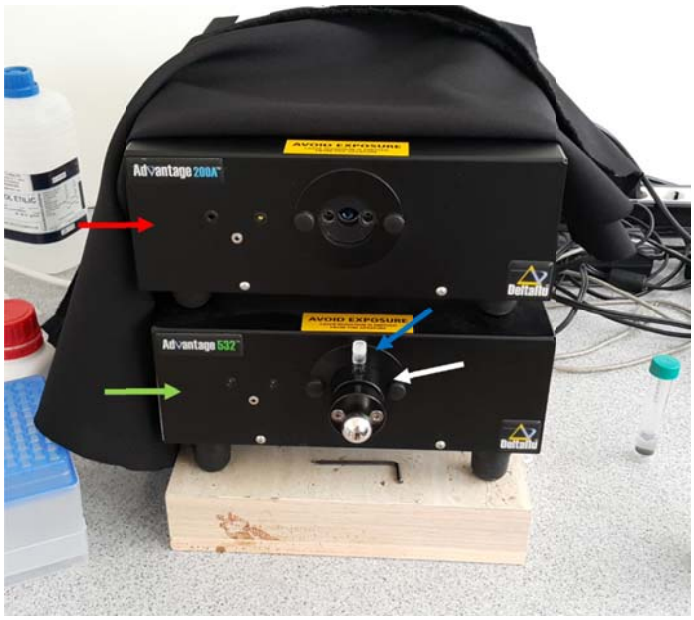

Figure 4. DeltaNU Advantage 532 compact dispersive Raman spectrometer. Upper unit of the device is equipped with a 632.8 nm laser line (red arrow), and the lower unit is equipped with a 532 nm laser line (green arrow). Samples are analysed within glass cuvettes (blue arrow) placed in sample holder (white arrow). The device is covered with black sheet during measurements to exclude signals from ambient light.

2.2. Obtaining and handling of the sea urchins

Sea urchins (*P. lividus*) were collected form Bay of Gruž in Dubrovnik city, Croatia. The collection was done from the shore using a handheld net. Sea urchins were taken from depth of about 0.5 metres. Immediately after collection the sea urchins were brought in a plastic box with sea water to the biological laboratories of the University of Dubrovnik. Sea urchins were obtained and handled in the same manner on three sampling occasions during the period of the present study.

2.3. Preparation of *Paracentrotus lividus* gonads for Raman analysis

Gonads were obtained on two sampling occasions by dissection of the sea urchins. One difference was that the first set of gonads (termed „Gonads 1“) was taken after the eggs were spawned from them, and the second set (termed „Gonads 2“) was taken without prior spawning. Another difference was in the time of obtaining: Gonads 1 were taken in mid-April, at the climax of *P. lividus* reproductive season (Tomšić et al,. 2010), and Gonads 2 were taken in the beginning of June, after the reproductive season. Carotenoids were extracted by keeping the gonads in ethanol (95 % purity) for one week in dark conditions, as in Cintă Pinzaru et al. (2015).

To extract carotenoids from gonads for the purpose of analysis, all, whole, gonads from the same sampling occasion were placed together in a small vial containing 5 ml of ethanol (95 % purity). However, the male and female gonads from Gonads 1 set were separated into two vials. The vials were kept in dark conditions to exclude possible photodegradation of carotenoids. The extraction lasted 7 days, after which time the supernatant from each extraction vial was transferred into another respective vial. This was done to obtain one-week extracts, and the solution fron these newly filled vials was used in further analysis.

For the Gonads 1 set, only the ethanol extract of gonads from both females and males was analysed. For the Gonads 2 set, only the female gonads were analysed, but both the ethanol extract and the gonad tissue after extraction. To prepare dried *P. lividus* gonad extracts for analysis on the Renishaw InVia Reflex Raman microscoe, the ethanol extract was dropped on the glass microscope slide. We waited until ethanol evaporated and analysed the dry layer of extracted matter by three laser lines: 532, 632.8 and 785 nm. Two pieces of tissue from Gonads 2 set (of the volume of ≈ 2 mm^3) were taken out of their extraction vials using tweezers and placed on a glass microscope slide. A coverslip was placed on the pieces of gonads in an attempt to keep their upper surface as planar as possible, to make it easier to get a good microscope focus.

The Renishaw InVia Reflex Raman confocal microscope was used to acquire Raman spectra from dried extracts of *P. lividus* gonads. A cobalt diode pumped solid state (DPSS), air cooled laser provided the 532 nm excitation line, He-Ne laser provided the 632.8 nm excitation line, and a diode laser provided the 785 nm

excitation line. Spectra were acquired with the spectral resolution of 0.5 cm^{-1} in the range from about 60 to 1830 cm^{-1} with the 532 nm laser line, about 590 to 1730 cm^{-1} with the 632.8 nm laser line, and from 720 to 1810 cm^{-1} with the 785 nm laser line. The WiRE^{TM} 3.4 software (Renishew, United Kingdom) was used for acquisition of spectral data, and Origin 6.1 software (OriginLab, USA) was used for processing of the data.

The acquisition conditions will be described only for the 532 nm laser line, as it was the only one that provided relevant spectra. Both female and male gonad extracts from the Gonads 1 set were analysed under following conditions: 1 s integration time, 5 acquisitions per spectrum, 20 mW laser power, and 20x objective. A different kind of experiment was conducted on gonad extracts from Gonads 2 set: all spectra were acquired with 1 s integration, 1 acquisition, 20x objective, but using progressively increasing laser power, from 0.1 mW up to 200 mW. There was a suspicion, based on the study of Kish et al. (2015), that lower laser power might clearly reveal multiple components of the v_1 carotenoid band.

2.4. Artificial spawning and preparation of eggs for analysis

Artificial spawning was done according to method by Tshushima et al. (1997), with slight modifications. In short, sea urchins were injected with about 2 ml of 0.5 M KCl dissolved in distilled water through the peristomal membrane into the coelomic cavity. Spawning was done in the laboratory on frist sampling occasion (in April), and on site of sea urchin collection on third sampling occasion (in June). The exact volume of the solution to be injected into each individual was estimated according to the size of the respective individual. At the onset of gamete release, three females were placed onto their respective beakers filled with natural sea water with their aboral side down. Females were removed after releasing enough eggs in order to avoid the last portion of eggs to be spawned, which may be of lower quality. The eggs from the three beakers were transfered into three respective glass vials and immediately cooled to 4 °C. Each vial contained 0.5 ml of eggs and 5 ml of natural seawater.

Upon arrival to Raman spectroscopy laboratory, eggs were promptly prepared for analysis on Renishaw Raman microscope. One droplet containing some eggs from the bottom of each vial (each droplet representing one of the three females) was transferred to a hydrophobic spectRIM^{TM} platelet (Tienta Sciences Inc.). We proceeded with analysis as soon as the water from droplets evaporated. Figure 5 shows some details of the procedure.

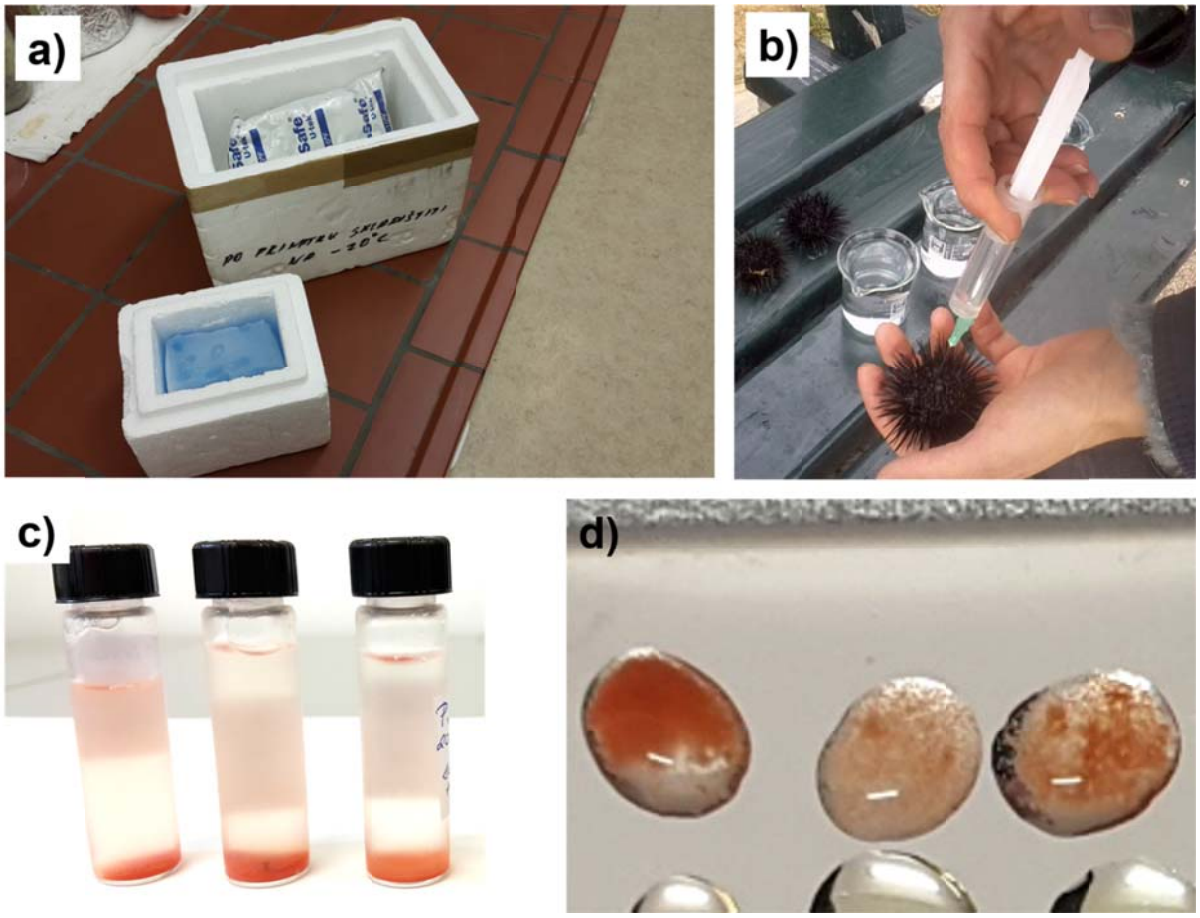

Figure 5. Details of preparation of *Paracentrotus lividus* eggs for Raman analysis. a) polystyrene box with cold packs used for transporting of the eggs at low temperature, b) artificial spawning of *P. lividus* individual, c) vials containing *P. lividus* eggs, d) fresh droplets with *P. lividus* eggs.

Analysis properties of Renishaw Raman microscope system were described in sections 2.1. and 2.3. The 532 and 785 nm laser lines were used for analysis of eggs. Raman information was acquired at several focal depths within the 1 to 3 eggs from each of the three females. The acquisition conditions for single spectra were: 1s integration, 1 acquisition, 2 mW and 20x magnification objective for the 532 nm laser line, and 2 s integration, 5 acquisitions, 30 mW and 20x for the 785 nm laser line.

The 532 nm laser line was used for Raman imaging. The spectra for the image were acquired under StreamLine^{TM} imaging setup, in only one focal plane, the focus being on the surface of the eggs. In short, the Raman images were created according to the following procedure: firstly, a rectangular area of interest to be analysed was defined on the live video image, encompassing the egg and its immediate surroundings. The size of the area was 1191 pixel in x axis and 431 pixel in y axis. In the measurement parameters we defined the spectral range by setting 1000 cm^{-1} as the centre, which resulted in automatic setting of the range from about 60 to 1830 cm^{-1}. The exposure time for one fow of pixels was 7 s, which means that the exposure time of each individual pixel was about 0.006 s. Raman images of carotenoid signal distribution were created applying the „intensity at point“ criterion to v_1 and v_2 carotenoid bands. WiRE 3.4 software was used for obtaining and storing spectral data, and Origin 6.1 software was used for processing of data.

2.5. Culture and sampling of *Paracentrotus lividus* larvae

Sea urchins were spawned according to the procedure described in section 2.4. The only difference was that we also took the “dry spermatozoa”. This means that the spermatozoa were taken with a micropipette directly from the spawning male`s aboral side, without getting them into contact with any liquid. This is done to prevent premature activation of spermatozoa motility, and so preserve the quality of sperm until fertilization. Eggs from two females were firstly suspended in 500 ml of filtered (1 µm filter), sterilized sea water. Fertilization was done by releasing the spermatozoa from the micropipette into the egg suspension and gently stirring the suspension for one minute.

Embryos, and later larvae, were cultured in a static system, in 10 l of filtered (1 µm filter), sterilized sea water in a glass container. Aeration for oxygen supply and mixing of water was supplied by an air pump, and the temperature was maintained at 26 ± 1 °C by an air conditioning device. Development of larvae was inspected twice a day using a microscope. Larvae were cultured till 48 h after fertilization, after which time they were filtered through a nylon net (50 µm). The whole culture volume was concentrated to 200 ml, and divided into 4 sample bottles. 50 ml of concentrated larvae solution was mixed with additional sea water in ratio 1:1 v/v and immediately

frozen. The second 50 ml aliquot was mixed with formalin (5 % solution) in ratio 1:1 v/v. Another 50 ml aliquot was mixed with paraformaldehyde (15 % solution) in ratio 50 ml larvae + 35 ml paraformaldehyde. Finally, the last 50 ml aliquot was mixed with glutaraldehyde (2.5 % solution) in the same ratio as with paraformaldehyde. The bottle with frozen larvae was transported in the polystyrene box, as was the case with eggs. Other bottles were transported at room temperature.

Larvae were analysed on Renishaw Raman microscope (described in sections 2.1. and 2.3.). Larvae were taken from the sample bottles using a pipette and the solution was dropped on a microscope slide. After water evaporation, larvae were found and their skeleton and body tissue was excited with the 532 nm laser line.

2.6. Obtaining the *Paracentrotus lividus* spines and their analysis

Spines were cut off using scissors from, or were shed by, dead sea urchins and were then placed into a plastic vial for keeping in dry conditions. Spines to be analysed were placed on a glass microscope slide and Raman information was acquired from several spots on the spine surface.

Analysis was done on the Renishaw Raman microscope, the properties of which have been described earlier (sections 2.1. and 2.3.). Both the 532 and the 785 nm laser lines were used to acquire Raman spectra. Spectra were acquired under 0.5 to 5 s int., 1 acq. 100x obj. and 2 to 200 mW laser power for the 532 nm excitation line. Spectra were then acquired under 3 s integration, 1 acquisition, 300 mW power and 100x objective using the 785 nm excitation line.

Scanning electron microscopy imaging was accomplished on a Hitachi SU8230 Cold Field Emission scanning electron microscope. A spine was adherently placed on Hitachi stub SEM holders (aluminium holder with M4 threads covered with carbon disc of 3 mm thickness). Samples were prepared for analysis by coating with 10 nm thick layer of gold.

2.7. *Paracentrotus lividus* pieces of digestive systems and intestine

Pieces of two digestive systems of *P. lividus* were taken from dissected sea urchins and placed into vials containing ethanol (95 % purity). The extraction followed the same procedure as described for gonads in section 2.3. Samples for SERS analysis were prepared in a glass cuvette by adding 5 µl of digestive system extract to 500 µl of AgNPs. The AgNPs were proivded by S. Cintă Pinzaru.

The extracts were analysed on DeltaNU Advantage 532 Raman spectrometer. Spectra were recorded within the 200 to 3500 cm^{-1} spectral range, with spectral resolution of 8 cm^{-1} using the 532 nm laser line. The acquisition conditions were: 5 s integration and 5 acquisitions. NuSpec softvare (Intevac, USA) was used for acquiring and storing the spectra.

2.8. Raman analysis of *Paracentrotus lividus* coelomic fluid

P. lividus coelomic fluid was sampled on first and on second sampling occasion. The samples are hence termed „C.fluid 1“ and „C.fluid 2“. Coelomic fluid was obtained either by taking the coelomic fluid from live sea urchins using a syringe, or by dissecting sea urchins and taking the coelomic fluid with a pipette. Coelomic fluid was placed into 5 ml vials and mixed with phosphate buffer (pH 7) in the ratio 1:1 (coelomic fluid : buffer).

Raman analysis of coelomic fluid samples was done on the Renishaw Raman microscope. Coelomic lfuid was prepared for analysis by dropping method, as described in section 2.3. We have excited the dry coelomic fluid with three laser lines – 532, 632.8 and 785 nm. However, the sample was fluorescent for the 632.8 and 785 nm laser lines, so only tha acquisition conditions for the 532 nm laser line will be described. Spectra were acquired under various conditions, with 1 to 5 s integraation time, 1 acquisition, 2, 10 or 20 mW laser power, and either 20x or 100x objective. Nevertheless, the resulting spectra of both C.fluid 1 and C.fluid 2 had the same features, and the intensity of spectra was comparable, so the samples were pooled.

2.9. Preparation of whole *Paracentrotus lividus* extracts

P. lividus individuals were meridionally dissected and all of their halves were placed in a sampling bottle containing ethanol (95 % purity). The purpose of this experiment was to probe if Raman spectroscopy could detect carotenoids in such a complex sample as an extract from all parts of sea urchin body combined. Extraction lasted 7 days, whereafter an extract stock solution was taken from extraction container. Extract was analysed both on Renishaw Raman microscope and on DeltaNU spectrometer, using only the 532 nm laser line on both devices.

Sample for Raman analysis on Renishaw Raman microscope was prepared by dropping method described in section 2.3. Aliquot for dropping was taken from the stock solution. The acquisition conditions were: 1 s integration, 1 acquisition, 2 mW laser power and 20x objective.

For analysis on DeltaNU spectrometer, an aliquot of 500 µl of the stock solution was transferred to a glass cuvette. The Raman analysis was done using the 532 nm laser line under 5 s integration and 5 acquisitions.

3. RESULTS

3.1. Raman analysis of *Paracentrotus lividus* gonads

The Raman spectra acquired from Gonads 1 are shown in Figure 6. This sampling occasion, where both male and female gonads have been sampled, gave us an opportunity to compare the carotenoids between the sexes. Although the Raman spectra were not clear enough to identify the carotenoid species, the three major carotenoid bands (v_1, v_2 and v_3) were present in all spectra. It seems that the extracted matter re-crystallized (Figures 6a and 6b). As seen in the Figure 6a, both the crystallized orange clusters and the background exhibited carotenoid signals, but orange clusters had much stronger bands, indicating that carotenoids were concentrated in the clusters.

When comparing Raman spectra from female (Figure 6c) and male (Figure 6d), the first thing to note is that spectra acquired from female gonads feature much stronger Raman signals than spectra from male gonads do. Another difference visible from our spectra is in the position of the v_1 band, which was centred around 1515.5 cm^{-1} in females, and around 1521.5 cm^{-1} in males. The v_2 and v_3 bands were on the same position in both male and female gonads.

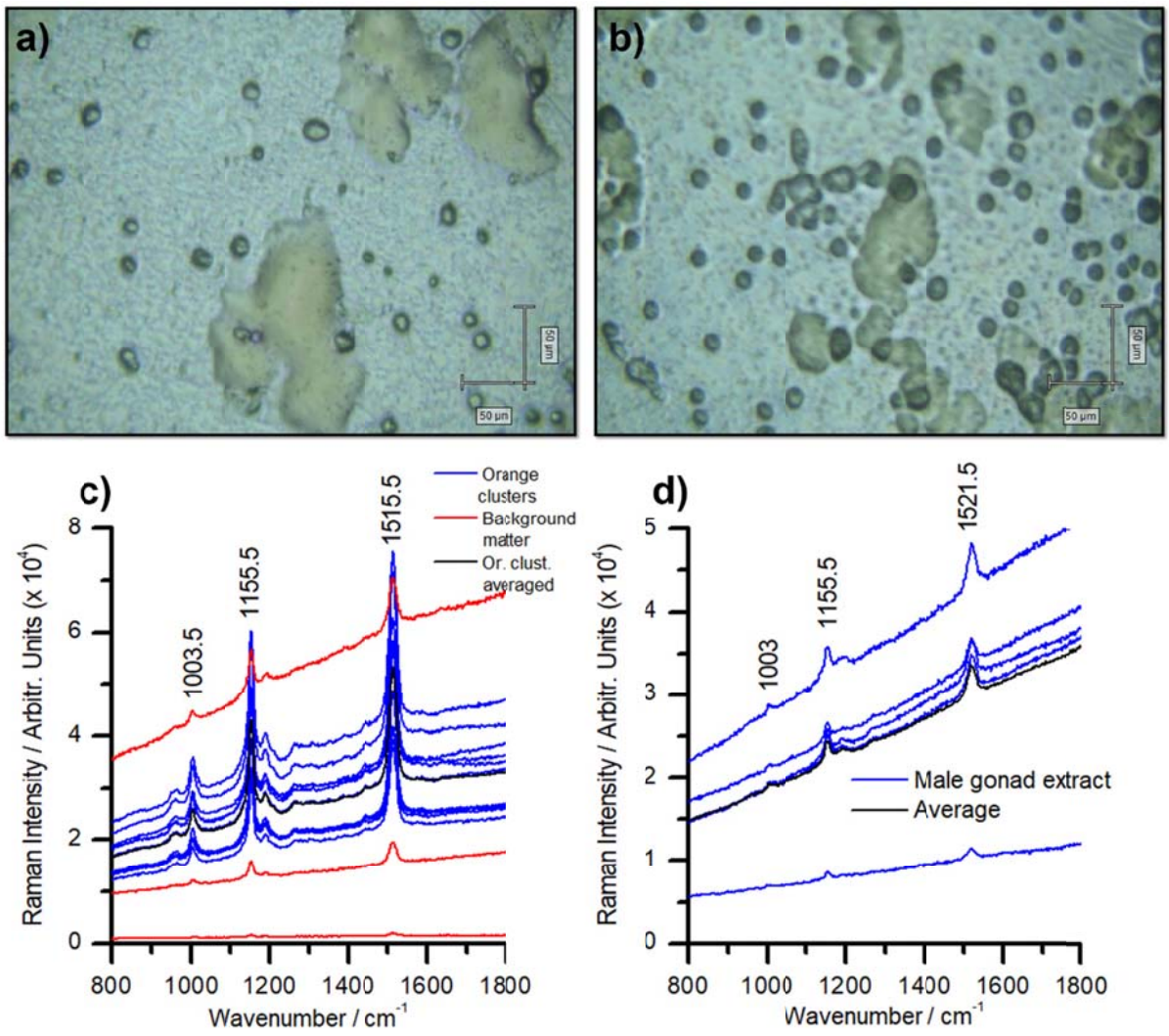

Figure 6. Micrographs and Raman spectra from *Paracentrotus lividus* gonad set „Gonads 1“. a) and b) Micrographs of female and male dry gonad extracts, respectively, taken under 20x magnification. c) and d) Raman spectra acquired from female and male dry gonad extract, respectively (excitation: 532 nm).

Carotenoid signals were detected both in ethanol extract and in the gonad tissue after extraction (Figure 7a). The difference in spectral features between the extract and the tissue, was in the position of the v_1 band (centred around 1510 cm^{-1} in extract and around 1511.5 cm^{-1} in tissue) and in its the shape and intensity.

The results of the increasing laser power experiment are shown in Figure 7b. Indeed, the asymetry and multi-component sturcture of the v_1 (which indicates the presence of more than one carotenoid species) was pronounced in cases where the extract was excited with 2 mW laser power or less. However, it can be observed

from the Figure 7b, that minor spectral features (i.e. lower intensity bands) were completely covered by noise when spectra were acquired with 2 mW or lwss, while they were clearly discernible in spectra acquired with 20 mW or more.

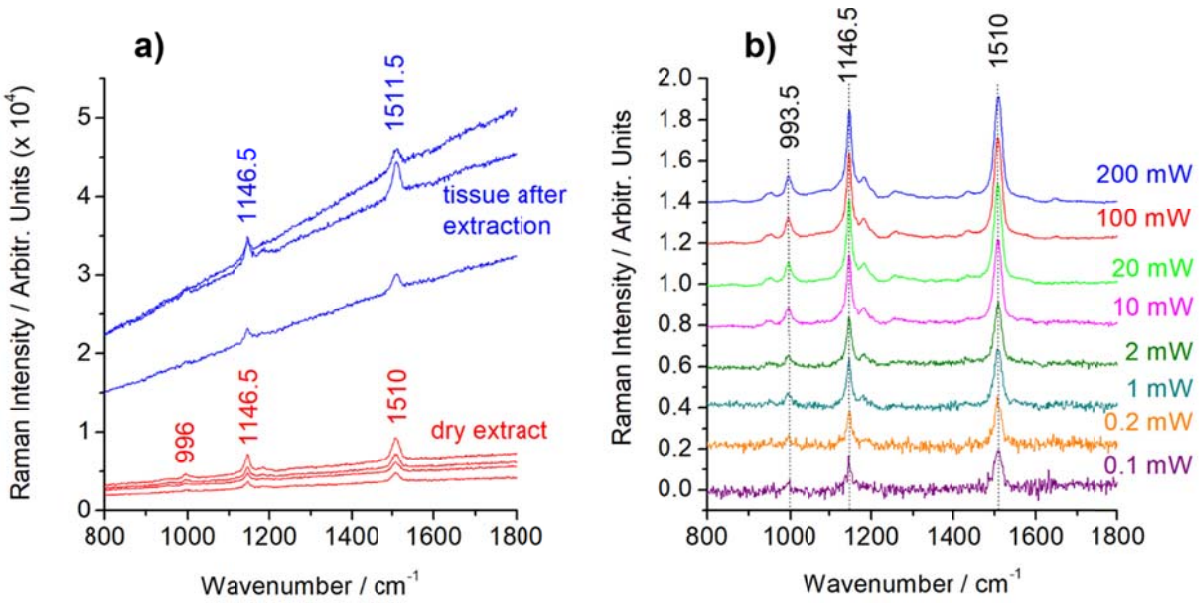

Figure 7. Raman spectra from *Paracentrotus lividus* gonads set "Gonads 2" acquired using the 532 nm laser line. a) Raman spectra acquired from dried gonad ethanol extract and the gonad tissue, b) Raman spectra acquired from dried gonad extract with increasing laser power, as indicated. Spectra in b) are normalised, their background was subtracted, and they were shifted along the y axis to allow better comparison. Every curve in b) is and average of three spectra.

3.2. *Paracentrotus lividus* eggs

Single-point spectra of eggs of *P. lividus* at various positions and focal depths within the cells acquired with the 532 nm laser line featured prominent carotenoid signals (Figure 8a). The ν_1, ν_2 and ν_3 bands were, on average, positioned at 1514.5, 1154 and 1003 cm^{-1}, respectively. There were small differences (about 1 or 2 cm^{-1}) in the positions of all bands in different spectra. Although there were differences in the absolute intensities of bands and background, spectra were reproducible and almost all spectra had the same Raman features. Judging by the presence of only one weak band past the 1550 cm^{-1} in most spectra, centred around 1579 cm^{-1}, we suggest that the spectra correspond to *β*-carotene. However, the 1200 to 1400 cm^{-1}

range does not quite match synthetic all-*trans*-*β*-carotene in terms of band positions, so we can not exclude the presence of other carotenoid contributing to final shape of the spectra.

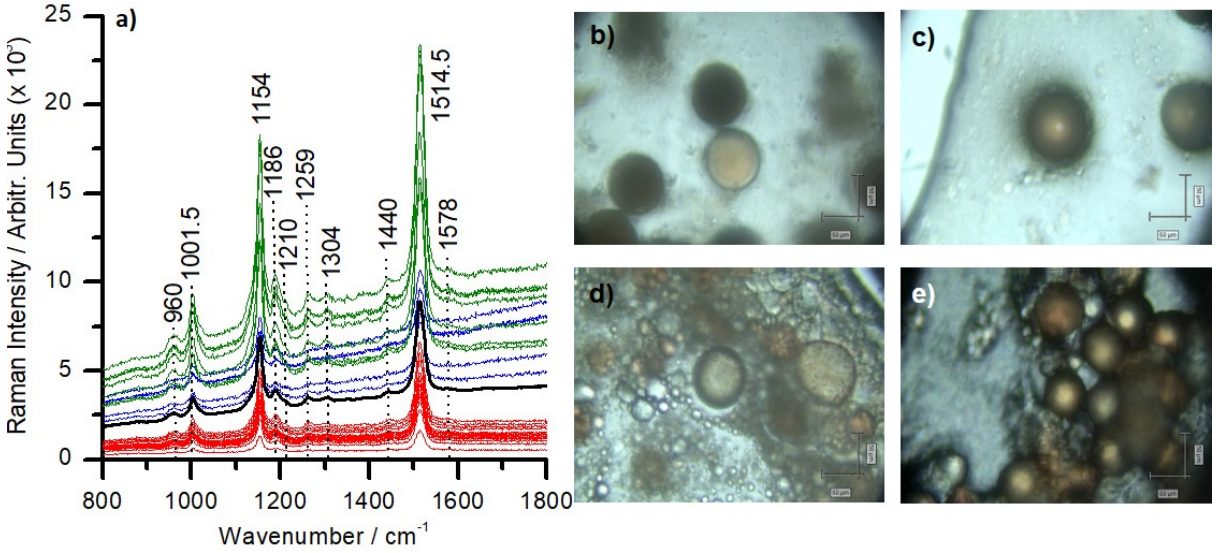

Figure 8. Raman spectra from *Paracentrotus lividus* eggs acquired using the 532 nm laser line, and the micrographs of the eggs. a) Raman spectra of eggs from three females. Different females are represented by three colours: red, green and blue. b, c), d) and e) micrographs of analysed eggs, taken under 200x magnification. b) and d) are focused on the top, c) and e) are focused near the equatorial plane.

Slight changes in carotenoid spectral features were observed in spectra acquired with the 785 nm laser line (Figure 9a). Firstly, the v_1 band shifted on average 1.5 cm^{-1} higher, from 1514.5 under 532 nm laser to 1516 cm^{-1} under 785 nm laser. The v_3 band also shifted by 1.5 cm^{-1}, from 1001.5 (532 nm) to 1003 (785 nm). The of v_2 band remained unchanged, but a band next to it appeared at about 1128 cm^{-1} under the 785 nm laser. The bands in the 1200 to 1400 cm^{-1} also experienced some preturbations. The bands centred around 1188, 1213 and 1304 cm^{-1} remained relatively unchanged in terms of their position. However, a band centred around 1334 cm-1 appeared in latter set of spectra, which was not observed in spectra acquired with the 532 nm laser line. The band centred aroumd 1440 cm^{-1} in the 532 nm spectra shifted to about 1443 cm^{-1} in the 785 nm spectra. The weak band centred around 1578 cm^{-1} was not visible in 785 nm spectra. A band centred around 1654 cm^{-1} also appeared in spectra acquired with the 785 nm laser line. This broad

band can be assigned to either amide I group of proteins (Rygula et al., 2013) or C=O stretching mode of lipids (de Gelder et al., 2007).

We also run measurements to attempt to localise the amine band (1654 cm^{-1}) and so try to get insights into protein distribution in eggs. We found that the carotenoids leached out of the eggs, as inferred by the presence of caroteniod bands also outside the eggs, but the proteins were largely retained within the eggs, concluded according to absence of amide I band outside egge (Figure 9b). However, the amide I Raman band distribution was uniform within individual eggs, so no more detailed information about protein localisation was obtained.

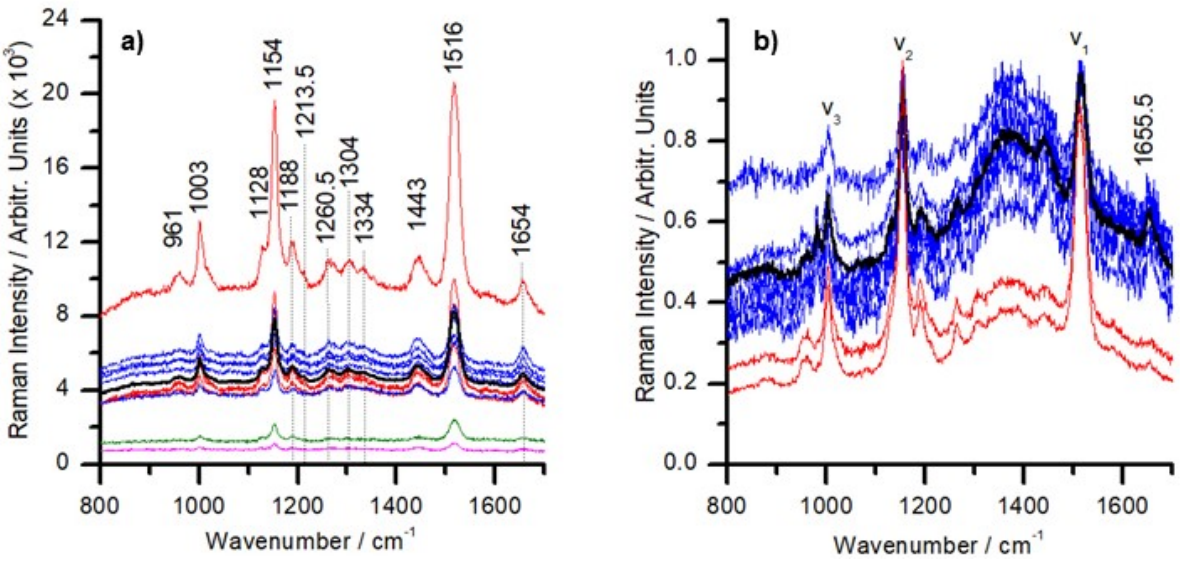

Figure 9. Raman spectra from *Paracentrotus lividus* eggs acquired using the 785 nm laser line. a) spectra acquired from eggs only. Red, blue, magerita and blue colour represent eggs from four different females. Black line is the average of all spectra. b) spectra acquired within the eggs (blue) and outside of eggs (red). Black line represents the average of spectra from within the egg only. Spectra in b) were normalised to allow comparison. Note the difference in amide I band around 1655.5 cm^{-1} intensity within and outside the eggs in b)

The Raman images depicting the distribution of carotenoids within the *P. lividus* eggs and the area around them (Figure 10) were drawn based on the intensity of v_1 and v_2 bands. The bands were centred around 1524 and 1164 cm^{-1}, respectively. We are not sure why it was shifted to higher wavenumber position in this particular measurement. The images showed the homogenous and uniform

distribution of carotenoids within the egg. The circular area of intense carotenoid signals on the image corresponds roughly to the physical shape and diameter of eggs, indicating that carotenoids are present both in endoplasm and cell cortex, and that there is no specific cellular organelle where carotenoids accumulate. The interferences from other focal planes did not hamper the imaging of these cells.

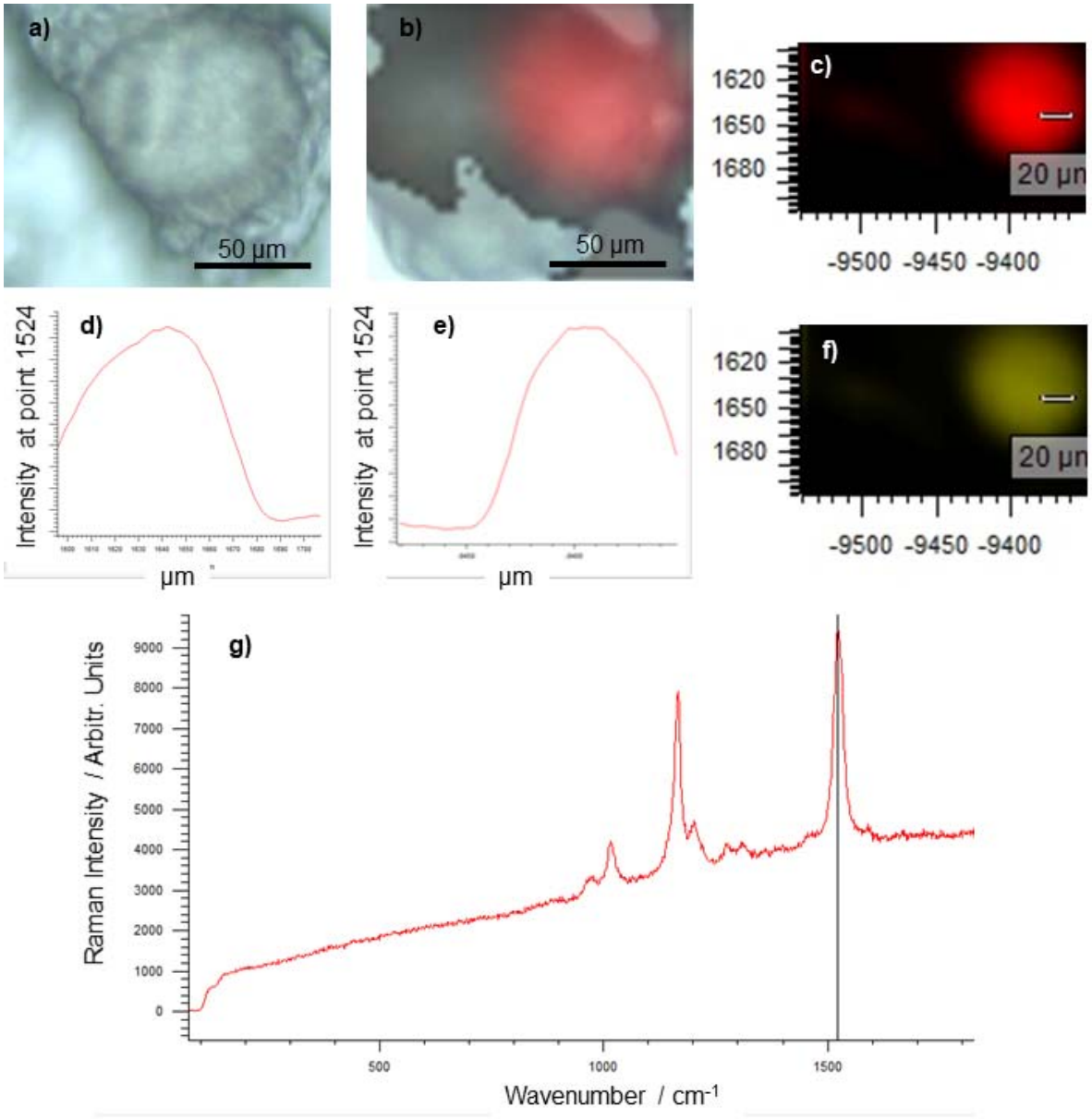

Figure 10. Data from a representative Raman imaging of a *Paracentrotus lividus* egg, acquired using the 532 nm laser line. a) a brightfield micrograph of the imaged egg, b) brightfield micrograph of the egg overlaid with its respective Raman image against the v_1 carotenoid band, c) Raman image of the *P. lividus* egg drawn against the v_1 carotenoid band, d) graph depicting the intensity of the v_1 band along the

vertical transect of the image passing through the centre of the egg, e) graph depicting the intensity of the v_1 band along the horizontal transect of the image passing through the centre of the egg, f) Raman image of the same *P. lividus* egg drawn against the v_2 carotenoid band, g) representative Raman spectrum at the crossing point of transects from d) and e).

3.3. *Paracentrotus lividus* larvae

Raman spectra were acquired from larvae preserved by freezing. Larva preserved in either of chemicals exhibited fluorescence for the 532 nm laser line. The larvae preserved by freezing were also in the best physical condition upon arrival to the laboratory, most probably because the ice held the larvae in position and prevented collisions with other larvae or the vessel walls.

The Raman spectra acquired from the bodies of larvae featured carotenoid signals, and many other signals which are not considered in this thesis (Figure 11c). Spectra were acquired both from random points in larval bodies and from red spots which are suggested here to be pigment-rich cells. The v_1, v_2 and v_3 carotenoid bands were centred around 1515, 1155 and 1005 cm^{-1}, respectively. A notable difference was, however, observed in the 1200 to 1400 cm^{-1} region, where the spectra from body of larvae featured two strong bands around 1307 and 1370 cm^{-1}, while spectra acquired from red spots featured three strong bands around 1307, 170 and 1430 cm^{-1}. This differences in Raman signals clearly indicate that this intensively red-coloured bodies have different molecular composition that the surrounding tissue.

Raman spectra of larval skeleton, acquired from the apexes and along body rods, generally featured signals of carotenoids or calcium carbonate, or even both in some cases (Figure 11a). The $CaCO_3$ signals correspond to calcite crystalline phase. The carotenoid signals may have been excited from the red spots along the skeletal rods, which may be carotenoid-rich cells taking part in synthesis of the growing larval skeleton (Figure 11b). The T, L, v_4 and v_1 calcite bands were centred around 158, 281, 711 and 1084 cm^{-1}, respectively, while v_1, v_2 and v_3 carotenoid bands were centred around 1514 or 1517.5, 1154 and 1004.5 cm^{-1}, respectively. It appears that larval skeleton is crystallized calcite phase already 48 hours after fertilization.

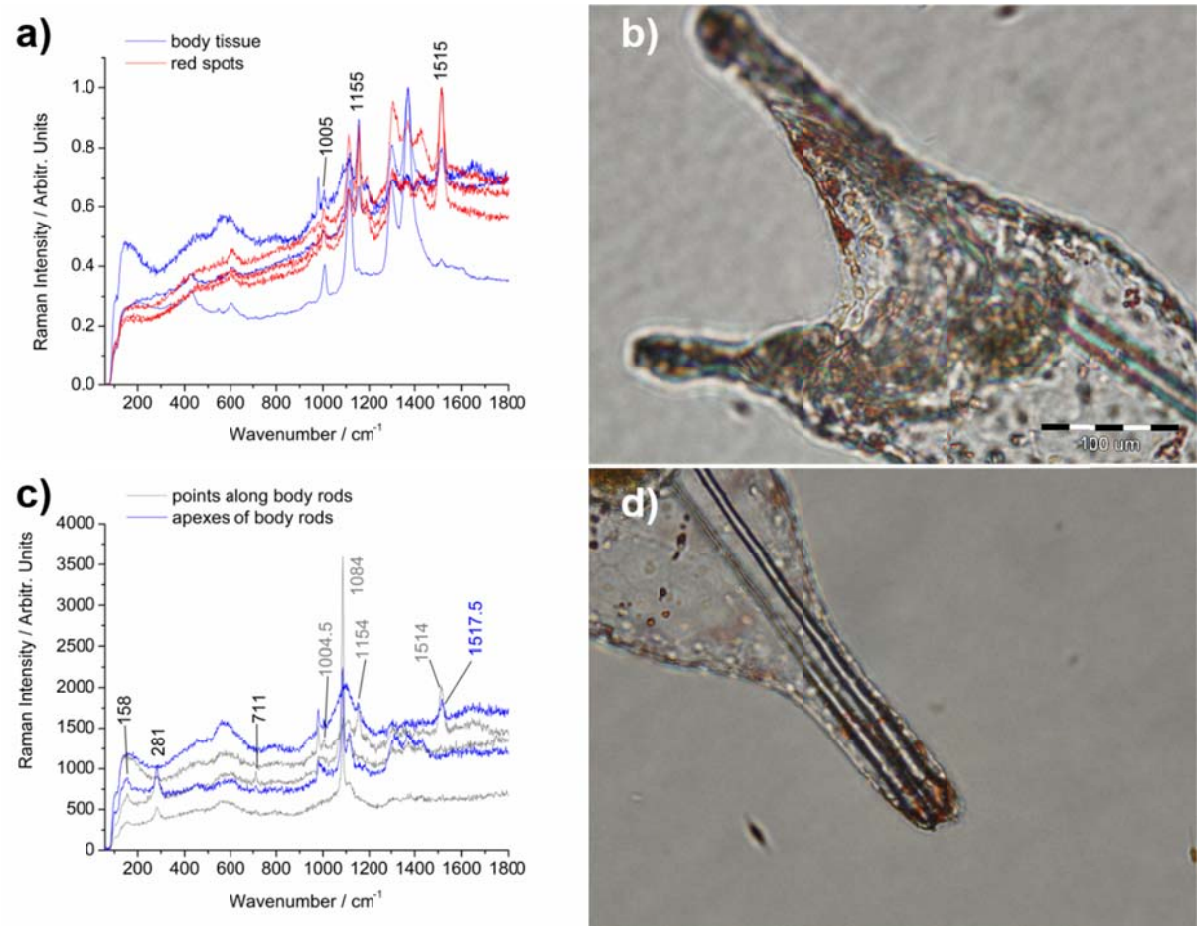

Figure 11. Raman spectra and micrographs obtained from *Paracentrotus lividus* cultured 48 days old larvae. a) Raman spectra acquired from points along body rods and from the rod apexes, b) micrograph of a larva focused on skeletal elements, c) Raman spectra acquired from larval body tissue and red bodies within the tissue, d) micrograph of a larva focused on red bodies within the larva. Excitation: 532 nm

3.4. *Paracentrotus lividus* spines

The Raman spectra acquired with 532 and 785 nm laser lines, and the micrographs of *P. lividus* spines are presented in Figure 12. Signals from calcium carbonate with calcite crystalline phase were present in all spectra acquired from lateral side of spines. The spectra acquired with 532 nm laser line, featured T, L, v_4 and v_1 bands of $CaCO_3$ centred around 154, 279, 711 and 1086 cm^{-1}, respectively. In addition, the 785 nm laser line excited two more low intensity Raman bands of calcite – the v_3 band around 1438 cm^{-1} and the $2v_2$ band around 1748 cm^{-1}.

This data suggest that the mineral component of *P. lividus* spine consists mainly of calcite. However, the properties of v_1 band are interesting. Firstly, it is asymetrical, particularly at its basal region. As outlined in the introduction, both v_1 band position and its width can be used as a measure of Mg incorporation. The position of the band in our spectra was at 1086 cm^{-1}, as in pure calcite, but it appears as having a shoulder band to the higher wavenumbers. Both Wang et al. (2012) and Perin et al. (2016) noted such asymetry of the v_1 band for both amorphous magnesian $CaCO_3$ and synthetic magnesian calcites, respectively. These researchers suggested that the v_1 band of magnesian $CaCO_3$ might in fact be a convolution of two (or more) bands. But, as stated before, apart from v_1 band broadening, all bands should be slightly shifted to higher wavenumber positions to qualify the minerals as magnesian calcites – which was not the case in our spectra. Taking into account everything said, the authors will not describe *P. lividus* spines as being mineralised with magnesian calcite at this point, but will denote it only as calcite. This issue requires further investigation to get a clearer picture of the spine mineral composition. The 785 nm laser line did not detect any asymetry of the v1 band, and it was centred around 1089 cm^{-1}.

We have analysed the spines under varying conditions in an attempt to get carotenoid signals in the spectra. Integration time, laser power and objectives were changed. The best results were obtained when the 100x magnification objective was used. Changing either integration time or laser power resulted in higher or lower overall signal intensity, but spectral features were, nevertheless, the same. Clear carotenoid Raman signals were not recorded.

Findings on *P. lividus* and *Arbacia lixula* spine morphology will be reported in more detail in a study by Cintă Pinzaru et al. (manuscript in preparation).

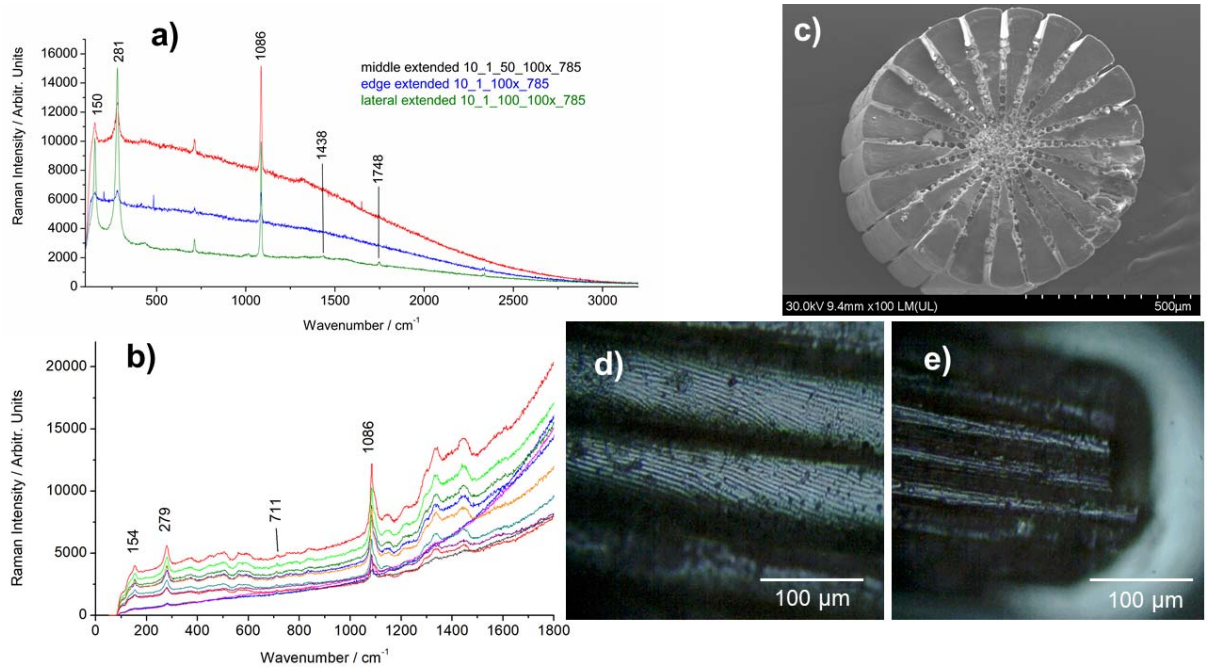

Figure 12. Raman spectra acquired from lateral side of *Paracentrotus lividus* spines using the a) 785 nm and b) 532 nm excitation lines. c) SEM image of spine cross-section, d) and e) lateral surface and tip of a spine, respectively, under 200x magnification..

3.5 Pieces of *Paracentrotus lividus* digestive systems and intestine

The SERS spectra of *P. lividus* digestive system extracts acquired using the 532 nm laser line seem to reflect fucoxanthin or its metabolic degradation products as major components (Figure 13). We can claim the presence of fucoxanthin and its geometrical isomers by a small band centred around 1609 cm^{-1}, which is characteristic for this carotenoid. The representative spectrum of pure fucoxanthin dissolved in ethanol from our other study (Cintă Pinzaru et al., manuscript in preparation) is added to the graph showing spectra of digestive system extracts for comparison. The position of the ν_1, ν_2 and ν_3 carotenoid bands in the spectra from pieces of digestive systems match those from pure fucoxanthin. However, the different shapes of the bands and the features in the 1100 to 1400 cm^{-1} region of digestive system extract spectra are slightly different from those of pure fucoxanthin, indicating the presence of other carotenoid species in lower quantities.

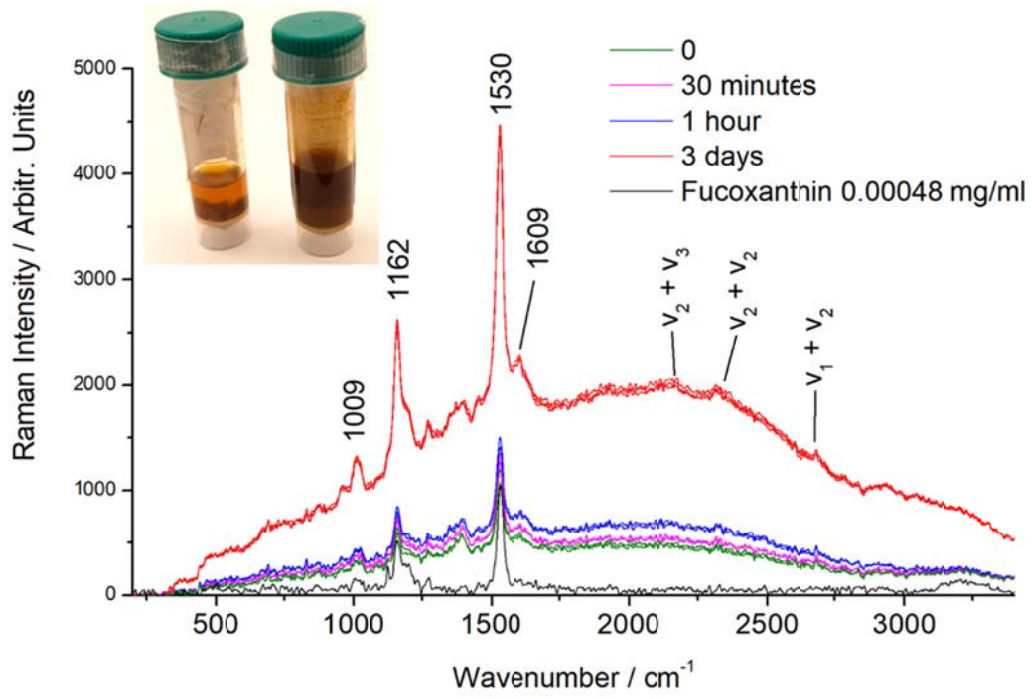

Figure 13. SERS spectra of *Paracentrotus lividus* digestive system extracts acquired using the 532 nm excitation line. The coloured lines represent measurements in time intervals (as indicated in graph legend) after adding 10 µl of *P. lividus* digestive system extract to 500 µl of Ag nanoparticles. The black line represents the spectrum of pure fucoxanthin dissolved in ethanol (0.00048 mg/ml). The inset shows the vial containing digestive system tissue during extraction.

3.6 Raman characterization of *Paracentrotus lividus* coelomic fluid

The dried coelomic fluid appeared as a mixture of various matter when observed under the microscope (Figure 14a). Both C.fluid 1 and C.fluid 2 had very similar Raman features (Figure 14b).The 532 nm laser line excited the three main carotenoid bands (v_1, v_2 and v_3) in dried coelomic fluid. However, the main carotenoid bands did not always appear as sharp bands, and their wavenumber positions varied about 15 cm^{-1} for the v_1 band and about 9 cm^{-1} for the v_2 band. This said, we suggest that coelomic fluid indeed contains carotenoids, and that there are several species of carotenoids there. Unfortunately, we could not localise the source of carotenoid signals because no clear outlines of any cells were visible in the

coelomic fluid when observed under the microscope. The matter containing the carotenoids could have clustered as in case of gonads, or otherwise aggregated.

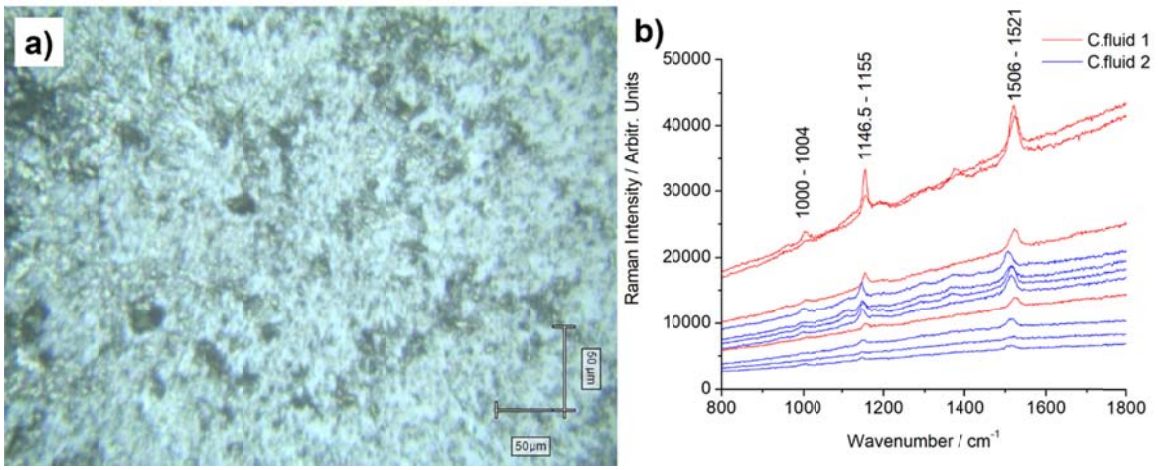

Figure 14. a) micrograph of dired coelomic fluid from sample C.fluid 1 under 200x magnification, b) Raman spectra acquired from *Paracentrotus lividus* coelomic fluid using the 532 nm laser line. Spectra from both C.fluid 1 and C.fluid 2 are shown.

3.8 Whole *Paracentrotus lividus* extract analysis

The whole sea urchin extract should comprise all of the cases described above and even more. But still, as with the previous cases, echinenone, *β*-carotene and fucoxanthin should be the major dissolved carotenoids. Carotenoid Raman signals were indeed detected in extracts of the whole *P. lividus*. Figure 15a presents the Raman spectra acquired on the Renishaw and DeltaNU devices. The main carotenoid signals (v_1, v_2 and v_3) appeared as wide, asymetrical bands above the high background.

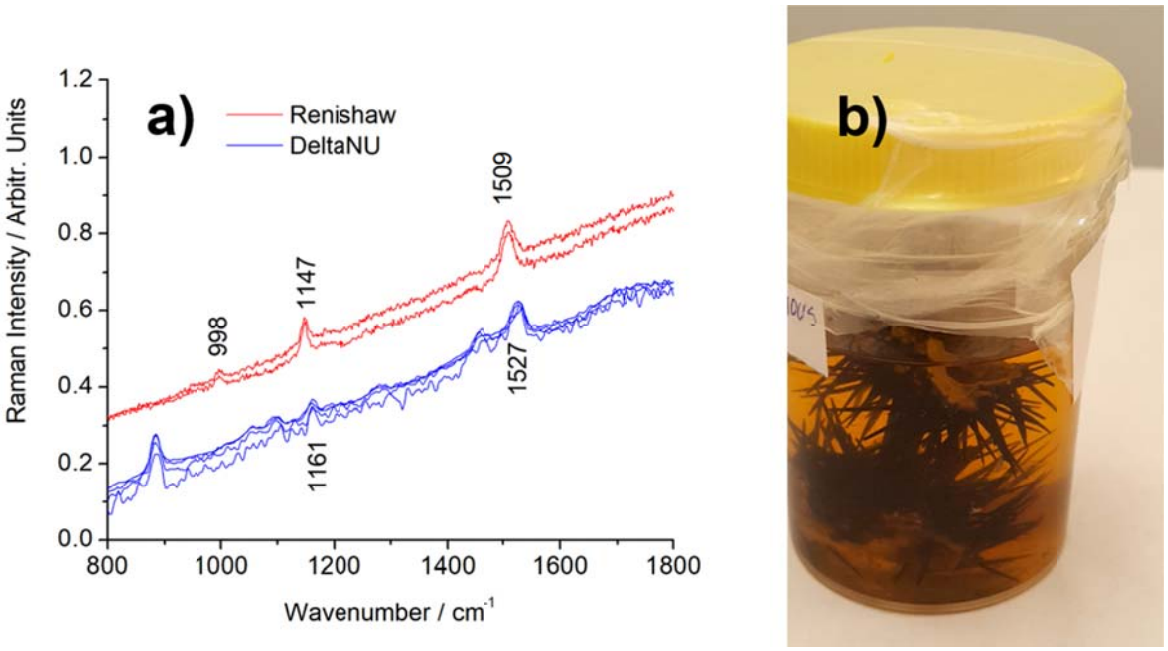

Figure 15. a) Raman spectra acquired from whole *Paracentrotus lividus* ethanol extract acquired with 532 nm laser line. Strong bands centred around 885 and 1450 cm^{-1} in DeltaNU spectra arise from ethanol. b) shows a bottle with whole *P. lividus* individuals immersed in ethanol during extraction.

4. DISCUSSION

4.1 *Paracentrotus lividus* gonads

Our results from Gonads1 suggest that the concentration of carotenoids is much higher in female than in male gonads, because the intensity of Raman bands is a good representation of the actual concentration of matter giving rise to that band (Cintă Pinzaru, pers. comm.). Furthermore, the position of v_1 carotenoid band differed between male and female gonads, being centred around 1515.5 cm^{-1} in females and around 1521.5 cm^{-1} in males. We feel confident to claim that this difference reflects different relative contribution of *β*-carotene and echinenone to the position of common band. Symonds et al. (2007) found that carotenoid profiles of *P. lividus* males and females can indeed be different, echinenone to *β*-carotene ratio being higher in males than in females in populations they studied. Our suggestion is further supported by the behaviour of the v_1 carotenoid band among carotenoid species with different lengths of their conjugated chains. The more double bond a polyene chain has, the lower will be the wavenumber position of the band. *β*-carotene has 11 double carbon=carbon bonds, while echinenone has only 9 double C=C bonds (Macernis et al., 2014). So, we can claim that our Raman graphs also reflect the higher content of echinenone relative to *β*-carotene in males, and vice versa in females.

The Gonads 2 set showed that carotenoids were not extracted completely from whole gonads after 7 days. Craft and Soares (1992) studied the solubility of *β*-carotene and lutein in various organic solvents. They showed that, even though the chemical stability of those carotenoids is fairly good in ethanol, their solubility in ethanol is only 30 and 300 mg/l for *β*-carotene and lutein respectively. This solubility value is small compared to some other solvent, like tetrahydrofuran, in which the solubility of β-carotene is as much as 10 000 mg/l. In this study, when extracting carotenoids from the tissue, we followed the simple extraction method also used by Cintă Pinzaru et al. (2015), who claimed to have determined the carotenoid concentration in *P. lividus* gonads using Raman spectroscopy to analyse the gonad ethanol extract. However, their concentration calculations may be invalid, since we proved here that there are still unextracted carotenoids in the gonads after 7-day

extraction. We suggest some kind of grinding or other kinds of micronising the tissue to be extracted to allow for better extraction.

Quantification of carotenoids in samples analysed in this study proved to be difficult, because of a number of factors, and this can well be a topic for another in-depth study. Ideally, carotenoids would be isolated from tissue and analysed in a solution, where the solvent would be an internal standard. However, there were issues with incomplete extraction of carotenoids, described in the previous paragraph, and the solvent itself, which features relatively low carotenoid solubility. On the other hand, if carotenoids would be quantified in the tissue itself (e.g. larval skeleton), there would be a question how deep does the laser excitation penetrate into tissue and how to determine the excited volume of the tissue. The problem of carotenoid quantification in marine organisms tissues will be addressed in another in-depth study.

In addition, we have shown in our laser intensity study, that using the lower laser power may provide additional data, because of the clear v_1 band asymetry when applying low power. The large noise in the spectra acquired with low laser power could be reduced by applying more acquisitions per spectrum and plotting the average as the final spectrum. On the other hand, high laser power better reveals minor spectral features of the dominant carotenoid species (e.g. bands in the 1100 – 1400 cm^{-1} region). Taking this into account, we would recommend to acquire spectra with both high and low laser power when analysing carotenoids in ethanol extracts, because both of them can give the information from different „angle“ which can be combined to draw a better picture of carotenoids in the sample.

Our spectra acquired from *P. lividus* gonads lack clear minor Raman bands that can be used to identify the carotenoid species. However, some information can still be inferred from the spectra. The most informative band is definitely C=C stretching mode usually centred between 1500 and 1520 cm^{-1}. Some additional characteristics of the band are its intensity above the background, number of peaks and full width at half-maximum (FWHM). If a large number of fresh *P. lividus* female or male gonads were measured, some correlations between their colour (Shpigel et al., 2007; Symonds et al., 2007; Symonds et al., 2009; Garama et al., 2012), pigment profile determined by HPLC and characteristics of the C=C stretching mode could be

established. This could be a direction in which to work on clarification of Raman pigment output from *P. lividus* gonads and enhance the Raman predictabillity of their pigment profile.

Meloni et al. (2016) raised the issue of fraudulent restaurants substituting a part of low-processed sea urchin gonads in food with similarly coloured egg yolk, and attempted to develop colorimetric method to discriminate between 100 % sea urchin gonads and gonads mixed with egg yolk. Raman spectroscopy could also be developed to serve this purpose, especially in cases where portable Raman instruments are available. Raman spectrum of egg yolk excited with 488 nm laser line was reported by Hesterberg et al. (2012) and features C=C stretching mode at 1525 cm^{-1}, and carotenoid compsition of egg yolk (Nimalaratne et al., 2013), although variable, is much different than the profile of *P. lividus* gonads. Thus, Raman spectroscopy could also be developed to serve to detect fraudulent products on sea urchin roe market.

4.2 *Paracentrotus lividus* eggs

The *P. lividus* egg really is a ball of carotenoids. Most of carotenoid bands, major and minor, were detected at all points within the egg using the 532 nm laser line, and even the carotenoids that leached out of eggs were readily detected. Carotenoid bands were well resolved even in spectra acquired using a non-resonant, 785 nm, laser line, albeit with some small perturbations of their positions. Furthermore, a Raman map of carotenoid distribution was successfully created using the 532 nm laser line. This is a good achievement given the sheer size of eggs, about 80 μm, and many focal planes when using the 20x objective. Thanks to the great abundance of carotenoids, even the outermost regions in the equatorial plane, which were not in focus at all, gave strong enough signals to produce an image of carotenoid distribution. It is known that sea urchin eggs comprise a lot of various intracellular compartments (reviewed by Schmekel, 1975). There is the cortical cytoplasm, which contains mostly cortical granules and yolk platelets, and the endoplasm, which contains the germinal vesicle and mostly endoplasmic reticulum, mitochondira and other. However, from our images, no localization of carotenoids to specific cellular organelles is observable.

4.3 Raman analysis of *Paracentrotus lividus* larvae

Monroy et al. (1951) investigated the total carotenoid quantity during *P. lividus* larval development. They found that initial egg quantity of carotenoids decreases from fertilization up to the gastrula stage, and therefrom gradually increases. To the best of authors` knowledge, no recent and precise study on the said topics exists. However, certain carotenoids ought to have important roles in sea urchin gametogenesis and further egg, embryonic and larval development. In support of this claim, Symonds et al.(2007) established that the total carotenoid content of *P. lividus* gonads decreases sharply after spawning, and the content of some individual carotenoids reach their peak values after spawning. Furthermore, Tsushima et al. (1997) showed that supplementing feed for adult *Pseudocentrotus depressus* with *β*-carotene and *β*-echinenone increases overall performance of larvae produced in subsequent spawning, whitle supplementing the feed with vitamin E results in no changes regarding the performance of larvae.

We recorded Raman signals of calcite in the 48-hour old larvae. However, our spectra have room for improvement, especially regarding the signal-to-noise ratio. Beniash et al. (1997) have detectad two phases of $CaCO_3$ in *P. lividus* larvae – calcite and amorphous $CaCO_3$ – using x-ray diffraction and infrared absorption spectroscopy. They suggest that the first pair of spicules that appear in the blastocoel are calcitic, and that they grow by deposition of amorphous $CaCO_3$ which is quickly transformed into calcite. Optimisationn of acquisition conditions in Raman spectroscopy, mainly increasing number of acquisitions per spectrum to reduce noise level and enhance clarity of bands, may reduce also reveal the amorphous phase of $CaCO_3$ alongside calcite.

4.4. Other *Paracentrotus lividus* tissues

Carotenoids have been identified by HPLC in sea urchin gonads (Liyana-Pathirana et al., 2002; Shpigel et al., 2006; Symonds et al., 2007; Symonds et al., 2009; Garama et al., 2012), the gut (Shpigel et al., 2006; Symonds et al., 2007; Symonds et al., 2009) and the coelomic fluid (Liyana-Pathirana et al., 2002). The carotenoid profile of these tissues is different, gonads being the richest in

echinenone, and fucoxanthin was found in relatively high quantities in the gut and the coelomic fluid. Shpigel et al. (2006) and Symods et al. (2007) suggested that the gut may be the major site of *β*-carotene metabolism in *P. lividus*, but this may not be true for fucoxanthin too, as it was described as a dominant carotenoid in coelomic fluid of *S. droebachiensis* by Liyana-Pathirana et al. (2002). We have detected carotenoids in all three mentioned tissues. However, the species-determinating carotenoid bands were not resolved enough to talk about exact carotenoid species, but the main carotenoid bands, especially the C=C stretching mode, were at different positions among tissues and among spectra from the same tissue. This means that Raman spectroscopy is able to detect multiple carotenoid species in these tissues. We suggest that the research of carotenoid metabolism could be done using Raman spectroscopy, but applying different acquisition conditions. For instance, a combination of low laser power with multiple acquisitions per spectrum, and also higher laser power could be a viable option.

In the present thesis, we demonstrated that Raman spectroscopy can indeed be used to study both carotenoids in soft tissues and mineral components of hard tissues of the stony sea urchin, *P. lividus*. An important advantage is that samples can be analysed in their native state, and so the best representation of sample composition can be obtained. However, the author`s current knowledge on the behaviour of carotenoid Raman signals in complex biological samples such as sea urchin tissues, does not allow for better identification of carotenoid species at this point. The method of acquisition of carotenoid signals should be improved, in part by following some suggestions outlined in the discussion above. The insights obtained in this thesis also open some new avenues for carotenoid research in marine invertebrates, and the thesis itself points out some issues that could be given more and focused attention.

5. CONCLUSION

We have analysed soft (gonads, eggs, larval tissue, digestive system) and hard tissues (larval skeleton) of the stony sea urchin, *Paracentrotus lividus* by Raman spectroscopy. In addition, *P. lividus* coelomic fluid and whole individual ethanol extract was characterised. Carotenoid presence was evidenced in the spectra acquired from all analysed soft tissues. Calcite was evidenced in analysed hard tissues – the larval skeketon and the spines – with the calcite in spines having highly ordered crystalline structure. Carotenoid species were identifyable in eggs and digestive system extract, as β-carotene and fucoxanthin, respectively. Carotenoid signals were also observed in Raman spectra acquired from gonads, coelomic fluid and whole sea urchin individual ethanol extract. The 532 nm laser line resonaltly excited carotenoid signals in all analysed soft tissues, while the 785 nm laser line proved to be useful for exciting signals from other, non-carotenoid, molecules in the samples which were not too fluorescent.

The pectra reported here are used for fires insights anddemonstration purpose Nevertheless, ueful information can still be extracted from these spectra, and four steps in carotenoid characterisation have been outlined in this study:

- *detection*: can be improved by optimisation of instrument spectral acquisition configuration
- *identification*: Multi-component Lorentzian fit could be applied to deconvolute carotenoid v_1 band to reveal C=C stretching modes from different carotenoid species, centred in range about 1510 – 1520 cm^{-1}, contributing to different extent to the overall v_1 band shape
- *Localisation*: the precision of Renishaw InVia Reflex Raman confocal microscope allowed us to probe the carotenoid comppsition of the sample on micrometre scale. This was especially useful in samples like *P. lividus* larvae and eggs.
- *Quantification*: the quantification of carotenoids in *P. lividus* tissues is possible, however, more knowledge and experience in analysis of carotenoids in marine organisms, and behaviour of carotenoids during extraction is necessary to conduct a precise carotenoid quantification.

6. REFERENCES

Ahel, M., Terzić, S. 1998. Pigment signatures of phytoplankton dynamics in the northern Adriatic*. Croat. Chem. Acta 71(2): 199 – 215.

Arizza, V., Giaramita, F.T., Parrinello, D., Cammarata, M., Parrinello, N. 2007. Cell cooperation in coelomocyte cyroroxic activity of *Paracentrotus lividus* coelomocytes. Comp. Biochem. Phys. A, 147, 389 – 394.

Behrens, G., Kuhn, L.T., Ubic, R., Heuer, A.H. 2013. Raman spectra of vateritic calcium carbonate. Spectrosc. Lett. 28(6): 983-995.

Beniash, E., Aizenberg, J., Addadi, L., Weiner, S. 1997. Amorphous calcium carbonate transforms into calcite during sea urchin larval spicule growth. Proc. R. Sec. Lond. B, 264: 461 – 465.

Boudouresque, C.E., Verlaque, M. 2013. *Paracentrotus lividus*. *In*: Lawrence, J.M. (Ed.) Sea urchins biology and ecology – Third edition. Developments in Aquaculture and Fisheries Science 38, 297 – 327.

Cintă Pinzaru, S., Müller, Cs., Tomšić, S., Venter, M.M., Cozar, B.I., Glamuzina, B. 2015. New SERS feature of β-carotene: consequences for quantitative SERS analysis. J. Raman Spectrosc. 46: 597-604.

Cintă Pinzaru, S., Müller, Cs., Tomšić, S., Venter, M.M., Brezestean, I., Ljubimir, S., Glamuzina, B. 2016. Live diatoms facing Ag nanoparticles: surface enhanced Raman scattering of bulk *cylindrotheca closterium* pennate diatoms and of the single cells. RSC Adv. 6: 42899 – 42910.

Cirino, P., Brunet, C., Ciaravele, M., Galasso, C., Musco, L., Fernández, T.V., Sansone, C., Toscano, A. 2017. The sea urchin *Arbacia lixula*: a novel natural source of astaxanthin. Mar. Drugs 15: 187 – 196.

Craft, N.J., Soares, J.H. 1992. Relative solubility, stability, and absorptivity of lutein and *β*-carotene in organic solvents. J. Agric. Food Chem. 40: 431 – 434.

Darvin, M.E., Sterry, W., Lademann, J. Vergou, T. 2011. The role of carotenoids in human peel. Molecules, 16: 10491-10506.

de Gelder, J., de Gussem, K., Vandenabeele, P., Moens, L. 2007. Reference database of Raman spectra of biological molecules. J. Raman Spectrosc. 38: 1133-1147.

de Nicola, M., Goodway, T.W. 1954. Carotenoids in the developing eggs of the sea urchin *Paracentrotus lividus*. Exp. Cell Res. 7: 23 – 31.

de Oliveira, V.E., Castro, H.V., Edwards, H.J.M. & de Oliveira, L.F.C. 2009. Carotenes and carotenoids in natural biological samples: a Raman spectroscopic analysis. J. Raman spectrosc. 41, 642-650.

Fernández-Boán, M., Fernández, L. & Freire, J. 2012. History and management strategies of the sea urchin Paracentrotus lividus fishery in Galicia (NW Spain). Ocean Coast. Manage. 69: 2265 – 272.

Flander-Putrle, V. 2010. Examples of high performance liquid chromatography (HPLC) application in marine ecology studies in the northern Adriatic. Natura Sloveniae, 12(1), 5 – 23.

Furesi, R., Madau, F.A., Palomba, A. & Pulina, P. (2014) Stated preferences for consumption of sea urchin: A choice experiment in Sardinia (Italy). *Proceedings in food system*.

Garama, D., Bremer, P., Carne, A. 2012, Extraction and analysis of carotenoids from the New Zealand sea urchin *Evechinus chloroticus* gonads. Acta Biophys. Pol. 59(1): 83 – 85.

Geetha, K., Umadevi, M., Sathe, G.V., Vanelle, P., Terme, T., Khoumeri, O. 2015. Surface enhanced Raman spectral studies of 2-bromo-1,4-naphthoquinone. Spetrochim. Acta A 138: 113-119.

Hesterberg, K., Schanzer, S., Patzelt, A., Sterry, W., Fluhr, J.W., Meinke, M.C., Lademann, J., Darvin, M.E. 2012. Raman spectroscopic analysis of the carotenoid concentration in egg yolks depending on the feeding and housing conditions of the laying hens. J. Biophotonics 5(1): 33 – 39.

Kaczor, A., Baranska, M. 2011. Structural changes of carotenoid astaxanthin in a single algal cell monitored in situ by Raman spectroscopy. Anal. Chem. 83: 7763 – 7770.

Katsikini, M. 2016. Detailed spectroscopic study of the role of Br and Sr in coloured parts of the *Callinectes sapidus* crab claw. J. Struct. Biol. 195: 1-10.

Kiokias, S., Proestos, C., Varzakas, T. 2016. A review of the structure, biosynthesis, absorption of carotenoids-analysis and properties of their common natural extracts. Curr. Res. Nutr. Food. Sci. 4(1): 25-37.

Kish, E., Mendes Pinto, M.M., Kirilovsky, D., Spezia, R., Pobert, B. 2015. Echinenone vibrational properties: from solvents to the orange carotenoid protein. Biochim. Biophys. Acta 1847: 1044 – 1054.h

Leruste, A., Hatry, E., Bec, B., De Wilt, R. 2015. Selecting an HPLC method for chemotaxonomic analysis of phytoplankton community in Mediterranean coastal lagoons. Transit. Waters Bull. 9(1): 20 – 41.

Liyana-Pathirana, C., Shahidi, F., Whittick, A. 2002. Comparison of nutrient composition of gonads and coelomic fluid of green sea urchin *Strongylocentrotus* droebachiensis. J. Shellfish Res. 21(2): 861 – 870.

Macernis, M., Sullskus, J., Malickaja, S., Robert, B., Valkunus, L. 2014. Resonance Raman Spectra and electronic transitions in carotenois: a density functional theory study. J. Phys. Chem. A 118: 1817 – 1825.

Matisori, S., Aggelopoulos, S., Tsoutsou, A., Neofitou, Ch., Soutsas, K., Vafidis, D. 2012. Economic value of conservation. The case of the edible sea urchin *Paracentrotus lividus*. J. Environ. Prot. Ecol. 13(1): 269 – 274.

Meloni, D., Spina, A., Satta. G., Chessa, V. 2016. A rapid colorimetric method reveals fraudulent substitutions in sea urchin roe marketed in Sardinia (Italy). Foods 5(3): E 47.

Meyers, K.J., Mares, J.A., Igo Jr, R.P., Truitt, B., Liu, Z., Millen, A.E., Klein, M., Johnson, E.J., Engelman, C.D., Karki, C.K., Blodi, B., Gehrs, K., Tinker, T., Wallace, R., Robinson, J., LeBlanc, E.S., Sarto, G., Bernstein, P., SanGiovanni, J.P. Iyengar, S.K. 2014. Genetic evidence for role of carotenoids in age-related

macular degeneration in the carotenoids in age-related eye disease study (CAREDS). Invest. Ophth. Vis. Sci. 55: 587-599.

Monroy, A., Monroy Oddo, A., De Nicola, M. 1951. The carotenoid pigments during early development of the egg of the sea urchin *Paracentrotus lividus*. Exp. Cell Res. 2(4): 700 – 702.

Nimalaratne, C., Wu, J., Schleber, A. 2013. Egg yolk carotenoids: composition, analysis, and effects of processing on their stability. *In*: Winterhalter, P., Ebeler, S.E. (eds.) Carotenoid cleavage products. American Chemical Society. p 238.

Nishino, H., Tohuda, H., Murakoshi, M., Satomi, Y., Masuda, M., Onozuka, M., Yamaguchi, S., Takayasu, J.,Tsuruta, T., Okuda, M., Khachik, F., Narisawa, T., Takasuka, N., Yano. M. 2000 Cancer prevention by natural carotenoids. BioFactors 13: 89-94.

Peng, J., Yuan, J., Wang, J. 2012. Effect of diets supplemented with different sources of astaxanthin on the gonad of the sea urchin *Anthocidaris crassispina*. Nutrients, 4: 922 – 934.

Perin, J., Vielzeuf, D., Laporte, D., Ricolleau, A., Rossman, G.R., Floquet, N. 2016. Raman characterization of synthetic magnesian calcites. Am. Mineral. 101: 2525-2538.

Pilbrow, J., Sabherwal, M., Garama, D., Carne, A. 2014. A novel fatty acid-binding protein-like carotenoid-binding protein from the gonad of the New Zealand sea urchin *Evechinus chloroticus*. PLoS ONE, 9(9): e106465

Schmekel, L. 1975. Egg and embryo ultrastructure. *In*: Czihak, G. (Ed.) The sea urchin embryo – biochemistry and morphogenesis. Springer Verlag Berlin Heidelberg New York, 1975, pp: 267 – 308.

Schulz, H., Baranska, M., Baranski, R. 2005. Potential of NIR-FT-Raman spectroscopy in natural carotenoid analysis. Biopolymers, 77: 212-221.

Shpigel, M., Schlosser, S.C., Ben-Amotz, A., Lawrence, A.L., Lawrence, J.M. 2006. Effects of dietary carotenoid on the gut and the gonad of the sea urchin *Paracentrotus lividus*. Aquacult. 261, 1269 – 1280.

Shumskaya, M., Wurtzel, E. 2013. The carotenoid biosynthetic pathway: Thinking in all dimensions. Plant Sci. 208: 58-63.

Singh, P., Singh, N.P., Yadav, R.A. 2010. Vibrational study on the molecular structure of 1,4-naphthoquinone and 2-methyl-1,4-naphthoquinone and their radical anions by using density functional theory. J. Chem. Pharm. Res., 2(6): 199-224.

Smith, W.E., Dent, G. 2005 Modern Raman spectopscopy – A practical approach. John Wiley & Sons, Ltd., p. 1 - 5.

Subramanian, B., Tchukanova, N., Djaoued, Y., Pelletier, C., Ferron, M. 2013. Raman spectroscopic investigations on intermolecular interactions in aggregates and crystalline forms of trans-astaxanthin. J. Raman Spectrosc. 44: 219 – 226.

Sugawara, T., Baskaran, V., Tsuzuki, W., Nagao, A. 2002 Brown algae fucoxanthin is hydrolyzed to fucoxanthinol during absorption by Caco-2 human intestinal cells and mice. J. Nutr. 132(5): 946 – 951.

Symonds, M.C., Kelly, M.S., Caris-Veyrat, C., Young, A.J. 2007. Carotenoids in the sea urchin Paracentrotus lividus: Occurrence of 9`-cis-echinenone as the dominant carotenoid in gonad colour determination. Comp. Biochem. Phys. B 148: 432 – 444.

Symonds, R.C., Kelly, M.S., Suckling, C.C., Young, A.J. 2009. Carotenoids in the gonad and gut of the edible sea urchin *Psammechinus* miliaris. Aquacult. 288: 120 – 125.

Tsushima, M., Kawakami, T., Mine, M., Matsuno, T. 1997. The role of carotenoids in the development of the sea urchin *Pseudocentrotus depressus*. Invertebr. Reprod. Dev. 32(2): 149 – 153.

Tsushima, M. 2007. Carotenoids in sea urchins. *In*: Lawrence (ed.) Edible sea urchins: biology and ecology. Elsevier Science B.V. p 159 – 166.

Umadevi, M., Ramasubbu, A., Vanelle, P., Ramakrishnan, V. 2003. Spectral investigations on 2-methyl-1,4-naphthoquinone: solvent effeces, host-guest interactions and SERS. J. Raman Spectrosc. 34: 112-120.

Wang, D., Hamm, L.M., Bodnar, R.J., Dove, P.M. 2012. Raman spectroscopic characterization of the magnesium content in amorphous calcium carbonates. J. Raman Spectrosc. 43: 543-548.

Wright, S.W., Jeffrey, S.W. 1987l Fucoxanthin pigment markers of marine phytoplankton analysed by HPLC and HPTLC. Mar. Ecol. Prog. Ser. 38: 259 – 266.

URL reference:

AZoM 2013 (https://www.azom.com/article.aspx?ArticleID=9854) Accessed: 28.08.201

DECLARATION

I declare under full responsibility that I have independently accomplished the present master thesis, using listed data sources and under professional supervision of supervisor doc. dr. sc. Sanje Tomšić and co-supervisor Conf. dr. Simona Cintă Pinzaru.

Fran Nekvapil